Photoinduced disinfection in sunlit natural waters: Measurement of the second order inactivation rate constants between E. coli and photogenerated transient species

Photoinduced disinfection in sunlit natural waters: Measurement of the second order inactivation rate constants between *E. coli* and photogenerated transient species

Efraim A. Serna-Galvis[a,b], Jean A. Troyon[a], Stefanos Giannakis[a], Ricardo A. Torres-Palma[b], Claudio Minero[c], Davide Vione[c,*], Cesar Pulgarin[a,]**

[a]*School of Basic Sciences (SB), Institute of Chemical Science and Engineering (ISIC), Group of Advanced Oxidation Processes (GPAO), École Polytechnique Fédérale de Lausanne (EPFL), Station 6, CH-1015 Lausanne, Switzerland*

[b]*Grupo de Investigación en Remediación Ambiental y Biocatálisis (GIRAB), Instituto de Química, Facultad de Ciencias Exactas y Naturales, Universidad de Antioquía UdeA, Calle 70 No. 52-21, Medellín, Colombia*

[c]*Dipartimento di Chimica, Università di Torino, Via P. Giuria 5, 10125, Torino, Italy*

**Corresponding Author: Prof. Dr. Davide Vione, E-mail: davide.vione@unito.it*

***Corresponding Author: Prof. Dr. Cesar Pulgarin, E-mail: cesar.pulgarin@epfl.ch*

Abstract

This work uncovers the implications of the estimation of exogenous inactivation rates for *E. coli* after the initial lag phase, and presents a strategy for the determination of the second-order inactivation rate constants (k^{2nd}) of these bacteria with relevant transient species promoted by solar light in natural waters. For this purpose, specific precursors were considered (nitrate ion, rose bengal, anthraquinone-2-sulfonate) as well as the

respective photo-generated transient species (i.e., hydroxyl radical (•OH), singlet oxygen ($^1O_2$) and triplet excited states). Under these conditions and by using suitable reference compounds (acesulfame K and 2,4,6-trimethylphenol in different series of experiments), the k^{2nd} values were obtained after developing a proper competition kinetics methodology. The k^{2nd} values were $(2.5\pm0.9)\times10^{11}$, $(3.8\pm1.6)\times10^{7}$ and $(1.8\pm0.7)\times10^{10}$ M^{-1} s^{-1} for the inactivation of *E. coli* by •OH, $^1O_2$ and the triplet state of anthraquinone-2-sulfonate (^{3}AQ2S*), respectively. The measurement of a reaction rate constant that is higher than the diffusion-control limit for small molecules in aqueous solution implies that bacteria behave differently from molecules, e.g., because of the large size difference between bacteria and the transients. The obtained k^{2nd} values were used for the modeling of the bacteria inactivation kinetics in outdoor systems (both water bodies and SODIS bottles), limited to the exponential decay phase that follows the initial lag time. Afterwards, the role of dissolved organic matter (DOM) as precursor of transient species for bacterial elimination was systematically studied. The interaction of different sunlight wavelength regions (UV-B, UV-A, blue, green and yellow light) with Suwannee river (SW) and Nordic Lake organic matter (ND) was tested, and the photoinduced disinfection exerted by DOM isolates (SW DOM, Suwannee River Humic Acid, Suwannee River Fulvic Acid or Pony Lake Fulvic Acid) was compared. It was not possible to achieve a complete differentiation of the individual contributions of DOM triplet states (^{3}DOM*) and $^1O_2$ to bacterial inactivation. However, the application of competition kinetics to *E. coli* under solar irradiation in the presence of SW led to a k^{2nd} value of $(2.17\pm0.40)\times10^{10}$ M^{-1} s^{-1}, which is very near the value for inactivation by ^{3}AQ2S* and suggests that the latter behaved very similar to SW-^{3}DOM* and was a good ^{3}DOM* proxy in the present case. The determination of the second-order inactivation rate constants of *E. coli* with •OH, ^{3}DOM* and $^1O_2$ represents a significant progress in the understanding of the external inactivation pathways of bacteria. It also allows predicting that, after the lag phase, $^1O_2$ would contribute to photoinactivation to a far lesser extent than •OH and ^{3}DOM*.

Keywords: Solar disinfection; Bacteria elimination; Water treatment; Competition Kinetics; Natural organic matter; DOM activation.

1. Introduction

The use of solar light as disinfecting agent (SODIS) is a technique applied in low-income countries to treat biologically polluted water from natural sources (such as lakes, rivers or wells) for drinking purposes (Fernàndez-Ibañez et al., 2017; Ndounla et al., 2014). This technique has been proved to efficiently eliminate a series of pathogenic bacteria responsible for enteric diseases (McGuigan et al., 2012). SODIS takes advantage of solar light ultraviolet constituents, which induce direct photochemical reactions on the DNA bases of the cells and/or the formation of reactive oxygen species (ROS) by excitation of intracellular photosensitizers (Giannakis et al., 2016b; McGuigan et al., 2012).

Solar irradiation can also promote disinfection by the generation of transient species through photosensitization of external substances that occur in water (e.g., nitrate ions and dissolved organic matter, DOM, (Giannakis et al., 2016b, 2016a; Romero-Maraccini et al., 2013; Romero et al., 2011; Rosado-Lausell et al., 2013; Vione et al., 2006). For instance, the photo-excitation of NO_3^- by sunlight produces the highly oxidative species •OH, which has documented disinfection capabilities (Eq. 1-2) (Mack and Bolton, 1999). Meanwhile, the interaction of sunlight with DOM can produce a singlet excited electronic state (Eq. 3), which through intersystem crossing (ISC) may evolve into a triplet state (^{3}DOM*, Eq. 4). The triplet state is a reactive transient and it can act as disinfecting agent for bacteria (Eq. 5) and viruses (Mattle et al., 2015), but the reaction of ^{3}DOM* with oxygen also produces singlet oxygen ($^1O_2$, Eq. 6). After its formation, $^1O_2$ can attack bacteria (Eq. 7) (Giannakis et al., 2016b; Sciacca et al., 2011).

$$NO_3^- + H_2O + sunlight \rightarrow \bullet OH + \bullet NO_2 + OH^- \quad (1)$$

$$\bullet OH + [E.\ coli] \rightarrow [E.\ coli]_{damaged} \rightarrow \rightarrow \rightarrow [E.\ coli]_{inactivated} \quad (2)$$

$$^1DOM + sunlight \rightarrow {}^1DOM^* \quad (3)$$

$$^1DOM^* \xrightarrow{ISC} {}^3DOM^* \quad (4)$$

$$^3DOM^* + [E.\ coli] \rightarrow [E.\ coli]_{damaged} \rightarrow \rightarrow \rightarrow [E.\ coli]_{inactivated} \quad (5)$$

$$^3DOM^* + {}^3O_2 \rightarrow {}^1DOM + {}^1O_2 \quad (6)$$

$^1O_2 + [E.\ coli]_{damaged} \rightarrow \rightarrow \rightarrow [E.\ coli]_{inactivated}$ (7)

The interaction between bacteria and transient species (i.e., •OH, ^{3}DOM* or $^1O_2$) has been analyzed in a qualitative way (Giannakis et al., 2016b; Ndounla et al., 2014; Sciacca et al., 2011; Spuhler et al., 2010), but quantitative information such as the second order rate constants (k^{2nd}) for the inactivation of the bacteria by the transient species is scarce. Works on the apparent first-order degradation kinetics for 8 types of bacteria under sunlight irradiation have been established, but unfortunately the second-order rate constants have not been assessed (Maraccini et al., 2016a; Maraccini et al., 2016b). It would be very useful to know the k^{2nd} values for bacterial inactivation because, differently from the first-order rate constants that strongly depend on the experimental conditions and are laboratory-dependent, the second-order ones allow for generalizations (Bodrato and Vione, 2014).

Additionally, although it is well-known that DOM plays an important role during the SODIS process (Giannakis et al., 2016b; Ndounla et al., 2014; Sciacca et al., 2011; Spuhler et al., 2010), the literature has few studies seeking to understand the interaction of sunlight components with DOM. More specifically, very little is known on how the origin and concentration of dissolved organic matter influence bacterial disinfection (Nguyen, 2015; Sinton et al., 2002). While the knowledge-base on viruses is significantly higher on aspects such as the photo-generation of transients (Kohn and Nelson, 2007), reactivity (Silverman et al., 2015) and effectiveness on different strains (Fisher et al., 2011; Romero-Maraccini et al., 2013), the complexity of bacterial pathogens has not allowed for significant knowledge advancements.

Therefore, this work was focused on the following aspects that merit investigation as indicated by the absence of relevant studies: *1)* the k^{2nd} determination for *E. coli* (as model bacterial pathogen) with the photo-generated transient species, using sunlight and nitrate anion (as •OH source (Mack and Bolton, 1999)), anthraquinone-2-sulfonate (AQ2S, the triplet state of which was here used as a proxy of ^{3}DOM* (Loeff et al., 1984; Maddigapu et al., 2010)) and rose bengal (RB, a well-known $^1O_2$ source (Kochevar and Redmond, 2000)); *2)* The modeling of the bacteria inactivation kinetics in outdoor systems (both water bodies and SODIS bottles) using the determined k^{2nd}; *3)* the systematic study of DOM activation with different sunlight components (i.e., UV-B, UV-A, blue light, green light and yellow light) for *E. coli* elimination and the evaluation of the effects that the

amount and type of DOM (Suwannee river organic matter, Nordic Lake organic matter, Suwannee river humic acid, Suwannee river fulvic acid and Pony lake fulvic acid as transient species generator) have on bacterial disinfection.

2. Methods and analyses

2.1 Chemicals and reagents

Sodium nitrate ($NaNO_3$, 99%), anthraquinone-2-sulfonate (AQ2S, 98%), rose bengal (RB), sodium chloride (NaCl, 99.5%), potassium chloride (KCl, 99%), plate count agar powder (PCA), acesulfame K (ACE, 99%), furfuryl alcohol (FFA, 98%) and 2,4,6-trimethylphenol (TMP, 97%) were purchased from Sigma-Aldrich. Acetonitrile (ACN, ≥ 99.8%) was obtained from Avantor. Suwannee river organic matter (SW, 2R101N), Nordic lake organic matter (ND, 1R108N), Suwannee river humic acid (SWHA, 2S101H), Suwannee river fulvic acid (SWFA, 1S101F) and Pony lake fulvic acid (PLFA, 1R109F) were provided by the International Humic Substances Society (IHSS). All solutions were prepared using Milli-Q water obtained from a Millipore (Elix) Merck Instrument.

2.2 Bacteria preparation and cultivability

Escherichia coli K12 (*E. coli*) from the "Deutsche Sammlung von Mikroorganismen und Zellkulturen" was prepared as described in our previous work (Giannakis et al., 2015) to produce a bacterial stock solution at 10^9 CFU mL^{-1}. In the reaction systems, the initial *E. coli* population was 10^6 CFU mL^{-1} obtained by dilution of the stock solution. From the reactor (*vide infra*), samples of 1.0 mL were periodically taken in sterile Eppendorf vials to do successive dilutions (using a saline solution containing 0.8% w/w NaCl and 0.08% w/w KCl), and 100 µL aliquots of the diluted systems were plated on plate count agar and then incubated (18-24 h at 37°C) for bacterial population determination. More details on the experimental procedure and handling can be found in Mangayayam et al. (2017) and Giannakis et al. (2018).

2.3 Reaction systems

2.3.1 Competition kinetics using specific precursors of transient species under simulated sunlight

Aqueous samples (100 mL) were placed in cylindrical Pyrex glass bottles that have a cut-off wavelength of 295 nm, with a diameter of 4 cm and a height of 7.5 cm. Irradiation experiments were carried out with an ATLAS SUNTEST CPS solar simulator, where the bottles were placed directly under the SUNTEST lamp and magnetically stirred at 750 rpm. Here, $NaNO_3$ was used as •OH source, AQ2S was chosen as a proxy compound for DOM, and RB was used as source of singlet oxygen ($^1O_2$). More information about these specific precursors of transient species is presented in Supplementary Material (Text SM1).

2.3.2. Light sources used for DOM excitation

The study of DOM interaction with the different sunlight components was carried out in homemade aluminum reflective boxes equipped with the corresponding lamps. The used UV-B source was an array of three 20 W Philips TL-D 01 UVB lamps with narrowband emission at 313 nm. For UV-A radiation it was used an array of three 18 W Philips TL-D BLB lamps with narrowband emission at 365 nm. The irradiation under blue light was done with three lamps Philips TL-D 18 W/18, and that under green light with three lamps Philips TL-D 18 W/17. The yellow light was generated by five Philips TL- D 18 W/16 lamps. Such conditions were chosen so as to obtain, for all of the lamps, an irradiance of 40 ± 2 W/m^2 over the irradiated solutions. The emission spectrum of each lamp can be found in Figure SM1. During the experiments, the bottles were placed directly under the lamps and the solutions were magnetically stirred with magnetic bars.

2.4 Analytical techniques

The irradiance spectrum produced by the specific lamps and the SUNTEST apparatus was measured using an USB2000+ spectrophotometer equipped with a pyranometer, which is able to measure irradiance from 300 to

2800 nm. The total organic carbon (TOC) content in the DOM solutions was determined using a Shimadzu Total Organic Carbon Analyzer (TOC-V_{CSN}). This analyzer was calibrated with standard solutions of potassium hydrogen phthalate. The UV-Vis absorption spectra of the DOM samples were measured with a Shimadzu spectrophotometer (UV-1800).

The time evolution of the chosen reference substrates (ACE, TMP and FFA) was monitored by HPLC using a HP Agilent 1100 series chromatograph equipped with a DAD detector and a Supelco C18 column (250 × 4.6 mm, 5µm). A summary of the chromatographic methods is presented in Table 1.

2.5 Competition kinetics calculations

The second-order reaction rate constant quantifies the interaction (reaction) of bacteria with transient species; this is useful quantitative information for generalization and kinetic analyses. To obtain the second-order reaction rate constants of *E. coli* with relevant transient species, the competition kinetics method was applied. This method uses reference compound(s) and takes advantage of its/their known reactivity with a given transient species (Mack and Bolton, 1999). Competition kinetics methodology is based on the simultaneous elimination and monitoring of both the reference compound and the target. Therefore, for the simultaneous degradation of a reference substance and of *E. coli* (our target), the second-order reaction rate constants (in M^{-1} s^{-1} units) of both the reference *compound* and the studied bacteria can be respectively expressed as follows: $k^{reference\ compound}_{transient\ species} = k^{1}_{reference\ compound}[transient\ species]$, and $k^{2nd} = k^{1}_{E.coli}[transient\ species]$. Here, k^1 represents the pseudo-first order decay constant of either the reference compound or the bacteria, and [transient species] is the steady-state (molar) concentration of the transient species.

In the simultaneous elimination of the reference and target compound, the two components occur in the same system and experience the same concentration of transient species. Therefore, one can reformulate the above equations as follows: $k^{reference\ compound}_{transient\ species} / k^{1}_{reference\ compound} = k^{2nd} / k^{1}_{E.coli}$. Experimentally, one monitors the elimination of both bacteria and the reference compound and obtains their pseudo-first order

decay constants (k^1). Then, the second-order rate constant (k^{2nd}) between the bacteria and the relevant transient species can be determined according to Eq. 8:

$$k^{2nd} = k^{reference\ compound}_{transient\ species} \frac{k^1_{E.coli}}{k^1_{reference\ compound}} \quad \text{(Eq. 8)}$$

The k^1 values are calculated as the slope from ln (X/X_o) vs. Time plots, elaborated with the experimental data. In the case of the reference compound, X_o and X denote the initial concentration and the concentrations at different treatment times, respectively. Similarly, for the *E. coli*, X_o and X are the initial bacteria concentration and the concentrations at different treatment times, respectively. The second-order reaction rate constant of the reference compound with the transient species ($k^{reference\ compound}_{transient\ species}$, units of $M^{-1}\ s^{-1}$) is usually available in the literature. For the reaction of bacteria with •OH, ^{3}AQ2S* and $^1O_2$, acesulfame K (ACE) was chosen as reference compound. ACE has second-order reaction rate constants $k^{ACE}_{\bullet OH} = (5.9 \pm 2.0) \times 10^9\ M^{-1}\ s^{-1}$, $k^{ACE}_{^3AQ2S^*} = (5.5 \pm 2.2) \times 10^8\ M^{-1}\ s^{-1}$, and $k^{ACE}_{^1O_2} = (2.8 \pm 1.1) \times 10^4\ M^{-1}\ s^{-1}$ (Minella et al., 2017). Meanwhile, for DOM as ^{3}DOM* source the reference compound was 2,4,6-trimethylphenol (TMP), which has a ^{3}DOM* reaction rate constant of $1.8 \times 10^9\ M^{-1}\ s^{-1}$ and a much lower reaction rate constant with $^1O_2$ ($6.3 \times 10^7\ M^{-1}\ s^{-1}$) (Halladja et al., 2007).

2.6 Modeling of the photoinduced inactivation of bacteria

The software APEX (Aqueous Photochemistry of Environmentally-occurring Xenobiotics) was here used to assess the photochemical inactivation lifetime of bacteria during the exponential decay phase that follows the initial lag time. The APEX software was used following the methodology described in the previous works of Bodrato and Vione, and Kohn *et al*. (Bodrato and Vione, 2014; Kohn et al., 2016). Further information on the modeling with APEX is presented in Text SM1.

3. Results and Discussion

3.1 *E. coli* disinfection by transient species generated with solar light

3.1.1 Bacterial inactivation by photo-generated transient species

The initial tests dealt with the ability of solar light to produce transient species from the precursors and to induce *E. coli* elimination as a consequence. To do so, the effect of different $NaNO_3$, AQ2S or RB concentrations on bacteria disinfection was considered, together with proper control runs (dark experiments as well as experiments under irradiation alone, without transient species precursors) (Figure 1). Solar light alone (at 600 W m^{-2} irradiance) induced a reduction of 2-log units of the *E. coli* population after 180 min of irradiation, while 10 mM $NaNO_3$ in the dark had practically no effect on bacteria during 180 min contact time (control experiment) (Figure 1A). However, the combination of sunlight with sodium nitrate accelerated significantly the elimination of bacteria, which can be associated to the generation of •OH and its subsequent reaction with *E. coli*. Figure 1A also shows that an increase of sodium nitrate concentration from 1 to 10 mM lowered the time required for complete disinfection, most likely due to a higher •OH production from the photolysis of more concentrated $NaNO_3$ (Eq. 1).

The *E. coli* inactivation by the solar-mediated excitation of anthraquinone-2-sulfonate is shown in Figure 1B. AQ2S in the dark (control experiment) did not produce bacteria elimination even after 240 min of contact. In contrast, the irradiation of 0.01 mM AQ2S resulted in an *E. coli* reduction (~ 3.5-log units) that was higher compared to that observed under solar light alone (~ 2.8 log units). This is coherent with a disinfection effect by ^{3}AQ2S*. The microorganism elimination was significantly enhanced by increasing the AQ2S concentration from 0.01 to 0.03 mM (Figure 1B). However, a further AQ2S increase up to 0.1 mM had a detrimental effect on bacterial inactivation, which became even lower than that observed with sunlight alone. Elevated AQ2S levels could cause self-competitive effects between excited states and the ground-state photosensitizer (Maddigapu et al., 2010), in addition to light shielding that can limit the direct action of radiation on *E. coli*.

Figure 1C shows the *E. coli* treatment under simulated sunlight in the presence of rose bengal (RB). Similar to the other photosensitizers, RB in the dark did not show disinfecting action but the RB-sunlight combinations

induced strong *E. coli* inactivation. A relatively low (1 μM) concentration of RB was enough to produce complete bacteria inactivation after 90 min irradiation. When the RB concentration was increased from 1 to 100 μM the inactivation rate was significantly enhanced. These findings highlight the ability of simulated sunlight to promote $^1O_2$ formation through RB excitation. Considering these results, 10 mM of $NaNO_3$, 0.03 mM of AQ2S and 10 μM of RB were selected as concentrations values of photosensitizers for the competition kinetics experiments.

3.1.2 Competition kinetics using the specific photosensitizers under simulated sunlight

ACE was selected as reference compound for the competition kinetics experiments, because it is non-toxic and it is not biodegraded by *E. coli*. Additionally, ACE does not undergo direct photolysis under sunlight and its second-order reaction rate constants with •OH, ^{3}AQ2S* and $^1O_2$ are known (Minella et al., 2017). Figure 2 reports the experimental results used to calculate the pseudo-first order rate constants resulting from the interaction between *E. coli* and the transient species. Note that in the case of the bacteria, the initial lag phase was not considered and only the exponential decay phase was taken into account. Eq. SM1 was used to calculate the second-order inactivation rate constant of *E. coli* by hydroxyl radicals ($(2.5 \pm 0.9) \times 10^{11}$ M^{-1} s^{-1}). By applying a corresponding procedure, the second-order inactivation rate constant between *E. coli* and ^{3}AQ2S* was calculated as $(1.8 \pm 0.7) \times 10^{10}$ M^{-1} s^{-1}. Finally, the interaction between *E. coli* and $^1O_2$ yielded the corresponding second-order inactivation rate constant ($(3.8 \pm 1.6) \times 10^7$ M^{-1} s^{-1}). A summary of these results is reported in Table 2 (bottom row).

It can be noted from the data in Table 2 that in all the cases the determined second-order rate constants of *E. coli* were higher than the respective ones with ACE. From a thermodynamic point of view bacteria are non-equilibrium systems (Desmond-Le Quéméner and Bouchez, 2014), thus they can either compensate for disturbances (the lag phase) or be easily affected by the attacks of reactive transient species, which produces fast reaction kinetics after the lag phase. It is also noticeable that k^{2nd} (*E. coli*, •OH) was much higher than the usually reported diffusion-control limit for aqueous solutions (~10^{10} M^{-1} s^{-1}) (Buxton et al., 1988). Actually, such limit is derived from the assumption that the two reactants are similar in size, which cannot clearly be the

case for a transient species and a bacterium. If the size difference is very large, the diffusion limit can be increased by even a couple of orders of magnitude (Desmond-Le Quéméner and Bouchez, 2014). Moreover, a bacterial cell could even incorporate some photosensitizer molecules, the photolysis of which would thus take place inside the cell and thereby circumvent the need for the two species to encounter by diffusion. Finally, the inactivation of bacteria under (simulated or natural) sunlight could be significantly enhanced by synergistic intracellular effects between UV-A, UV-B and internal photoinduced transient species. The synergy between UV-A and UV-B radiation has for instance been shown to induce faster inactivation than the sum of UV-A and UV-B provided separately (Buettner and Hall, 1987). The issue is that UV-A and UV-B radiations are able to damage the bacterial cell by means of different mechanisms that, taken together, in some circumstances could speed up the cell death. This effect is enabled by the very complex structure and functioning of a bacterium and cannot be operational with a simple molecule such as ACE.

On the other hand, the measured second-order inactivation rate constants with •OH, ^{3}AQ2S* and $^1O_2$ allow for modeling of the kinetics of the photoreactions involving •OH, ^{3}CDOM* and $^1O_2$ in sunlit surface waters, as well as in SODIS systems. The results of photochemical modeling by using the APEX software are reported in Figure 3 (first-order photoinactivation rate constant as a function of the dissolved organic carbon - DOC). Two cases are shown, of which one is representative of a natural water body (water depth d = 10 m, Figure 3A) and the other of a SODIS system (10 cm depth as for a water bottle placed over a roof, Figure 3B). The inactivation kinetics is obviously much faster (hours vs. days) in the more shallow system. In both cases •OH and ^{3}DOM* would be the main photoinactivation pathways for *E. coli*, while $^1O_2$ would play a negligible role. In particular, under the assumed conditions (0.1 mM nitrate and 1 μM nitrite as •OH sources, in addition to DOM) and in the water-body scenario, the inactivation with •OH would prevail for DOC < 4 ppm_C, and that with ^{3}DOM* for DOC > 4 ppm_C. An increase of the DOC is anyway detrimental to inactivation, because elevated DOC inhibits the •OH process to a higher extent than it enhances ^{3}DOM* (Minella et al., 2017). A similar behavior is observed in the SODIS system, but in this case the •OH/^{3}DOM* transition is observed at around 7 ppm_C. It is to be highlighted that the predicted inactivation is referred to the first-order process that follows the lag time, thus the actual inactivation may be considerably longer. In particular, because the inactivation lifetime is the time needed to just halve the number of bacteria, the achievement of effective disinfection in SODIS by •OH +

^{3}DOM* (indirect inactivation) would require much more than a day-long exposure. Considering that actual SODIS is considerably more effective than predicted here (McGuigan et al., 2012), it is clear that direct inactivation is very important inside a water bottle exposed to sunlight. The same is not necessarily true in a real water body, where the penetration of UV radiation (the most effective towards direct inactivation) in a water column of some meters is quite limited.

The modeling of DOM photoactivity was based on its total amount (measured as the DOC) and not on its source and type. The experiments that follow are aimed at elucidating the effect of different types of DOM on the photoinduced inactivation of bacteria, taking into account both the reaction pathways and the inactivation kinetics.

3.2 Systematic study of the effect of DOM on *E. coli* inactivation

3.2.1 Effect of the light type

For the evaluation of the effect of different solar light components on the *E. coli* inactivation in the presence of DOM, lamps emitting selectively UVB light, UVA light, blue light (BL), green light (GL) and yellow light (YL) were tested as radiation sources. A widely used reference DOM (Suwannee river DOM, SW) and a representative aquatic DOM (Nordic lake DOM, ND) (Semitsoglou-Tsiapou et al., 2016) at a moderate concentration (i.e., 2.0 ppm TOC) were considered. Control experiments for bacteria and DOM in the dark were carried out as well (Figure SM2).

Figure 4 presents the disinfection curves obtained by using the different light types in the absence and presence of ND or SW. Under the tested conditions, UV-B and UV-A by themselves (i.e., without DOM) produced a strong inactivation of *E. coli*, whereas BL, GL and YL had a low to negligible disinfection effect (see Text SM2). Through these control tests (i.e., DOM absence) one gets insight into the relationship between light-induced inactivation pathways and the bacterial and enzyme photo-reactivation processes (Giannakis et al., 2015; Rincón and Pulgarin, 2004; Thompson and Sancar, 2002). Comparing the bacteria population evolution with and without DOM, it can be noted that DOM particularly enhanced inactivation on the presence of UV-B

(for SW) and UV-A radiation (for both SW and ND). In contrast, the disinfection profiles of *E. coli* exposed to BL, GL or YL (solar light components with wavelength longer than 400 nm) either with or without DOM were very close (Figure 4). The UV-vis spectra of SW and ND (Figure SM3) suggest that these DOM types have their strongest absorptivity in the UV-A and UV-B regions, which is mainly associated to the presence of chromophoric moieties such as quinones and aromatic carbonyls (relevant groups in the formation of ^{3}DOM*) (Chen et al., 2002; Golanoski et al., 2012; Sharpless, 2012; Sharpless and Blough, 2014; Vione et al., 2014). This issue could explain the acceleration of *E. coli* disinfection in the presence of DOM irradiated by UV-A or UV-B light (Figure 4).

3.2.2 Effects of DOM type and concentration

For the effect of DOM concentration on *E. coli* inactivation, the experiments were carried out using UV-A light (see Text SM3). Figure 5 shows the *E. coli* evolution under UV-A irradiation with different concentrations (1.0, 2.0 and 5.0 ppm TOC) of ND or SW. For ND, the presence of 1.0 or 2.0 ppm TOC significantly enhanced the elimination of bacteria. However, at 5 ppm TOC the resulting disinfection was back at approximately the same level observed without DOM. In contrast, the addition of SW DOM at both 2.0 and 5.0 ppm TOC had an accelerating effect on the bacteria elimination. As is shown in Eqs. 3-7, DOM is able to produce transient species that can inactivate bacteria (Giannakis et al., 2016b; Ndounla et al., 2014; Sciacca et al., 2011; Spuhler et al., 2010) and this effect is higher as the DOM concentration increases. However, a large amount of DOM may induce a detrimental effect associated to the scavenging of photogenerated reactive species (most notably •OH) and the attenuation of light (Rodríguez et al., 2016).

Because DOM is largely made up of humic substances (i.e., humic and fulvic acids) (Rodríguez et al., 2016), in order to study the ability of these components to inactivate *E. coli*, Suwannee river humic acid (SWHA) and fulvic acid (SWFA) as well as Pony lake fulvic acid (PLFA) were also tested. The rationale for choosing SWFA (an allochthonous humic substance) and PLFA (an autochthonous humic substance) was to get insight into the role of the fulvic acid source on bacteria inactivation. Figure 5C compares the logarithmic reduction of *E. coli* population after 180 min of treatment with SW and different humic substances at variable

concentrations. It can be observed that SW enhanced disinfection as the TOC increased, while SWHA, SWFA and PLFA produced a disinfection peak at 1.0 ppm TOC. After the peak, bacterial elimination decreased as the TOC increased. The differences among the tested DOM samples and humic substances, including their different sources (Halladja et al., 2007) could be examined considering their optical and chemical characteristics (i.e., E_{365nm}, phenolic content and electron donating capacity; see Table 3, Figures SM3 and SM4), which affect their ability to produce transient species.

It can be noted that ND absorbs UV-A light to a higher extent than SW (see the E_{365nm} value). Are you sure that E365 has a molarity unit? How do you measure molarity for organic matter? It is rather $mgCL^{-1}$ or moles of carbon per liter? As a consequence, compared to SW, a lower ND concentration is required to have significant radiation absorption and produce a noticeable enhancement of *E. coli* inactivation. However, ND has also higher ability to screen light and inhibit photo-processes at high concentration (see Figures 5A and 5B). As far as humic substances are concerned, they are concentrated fractions of their respective DOM types (see IHSS web site, (International Humic Substances Society, 2018)). Therefore, the UV light absorption ability of SWHA and SWFA is stronger than SW as indicated by the E_{365nm} parameter (see Table 3). This means that low amounts of SWHA and SWFA may produce a similar effect as that of SW at higher concentrations (see Figure 5C).

Considering the data in Table 3, it can be observed that SWHA and SWFA have more phenolic moieties than SW. Because phenols are reducing agents, the electron donating capability (EDC) coherently follows the order SWHA ~ SWFA > SW (Walpen et al., 2016). It has been proposed that the radiation absorption of DOM in the near-UV region results primarily from intermolecular charge transfer between hydroxy/methoxy-aromatic electron donors (which could be phenols and/or methoxylated phenols) and carbonyl-containing electron acceptors (such moieties include quinones and/or aromatic ketones/aldehydes) (Sharpless and Blough, 2014). Hence, the higher phenolic moieties content and EDC of SWHA or SWFA compared to SW may explain their higher photo-activity, and the reason why a similar bacteria inactivation was achieved with lower SWHA or SWFA concentrations (1 ppm) compared to SW (5 ppm, Figure 5C). However, it should be indicated that a further characterization of DOM regarding the other photochemically relevant moieties (i.e., electron acceptors:

quinones and ketones), will provides additional information on differences among the DOM samples and humic substances.

On the other hand, one should consider that PLFA has more condensed aromatic groups than SWFA, and these groups promote the photochemical reactivity of PLFA (Sciacca et al., 2010). PFLA has also a higher amount of nitrogen than SWFA (International Humic Substances Society, 2018), and the functional groups containing N are very important for some photochemical reactions of fulvic acids (Bushaw et al., 1996; D'Andrilli et al., 2013). Therefore, although PLFA shows lower UV-light absorption than SWFA (Figure SM4), it is more effective in inducing bacteria disinfection (Figure 5C).

3.2.3 Competition kinetics using DOM as source of transient species

To complement the understanding of DOM reactivity toward *E. coli*, a competition kinetics was applied to systems that use UV-A light and SW or ND as sources of transient species (most notably, ^{3}DOM*, $^1O_2$ and •OH). The compound 2,4,6-trimethylphenol (TMP) at 0.05 mM initial concentration was used as ^{3}DOM* probe and reference substrate, because TMP reacts mostly with ^{3}DOM* (with second-order reaction rate constant $k_{^3DOM*}^{TMP}$ = 1.8×10^9 M^{-1} s^{-1}), while reactions with $^1O_2$ and •OH occur to a lesser extent (Semitsoglou-Tsiapou et al., 2016).

TMP is non-biodegradable (Pubchem, 2018), and a preliminary assessment showed that it has no significant toxic effects on *E. coli* even at 1.0 mM concentration (Figure SM5). The compound furfuryl alcohol (FFA) can be used as $^1O_2$ probe (Semitsoglou-Tsiapou et al., 2016), but unfortunately it cannot be used in competition experiments in the presence of bacteria because of its toxicity (Figure SM6). The overall rationale of the procedure here described is that the competition kinetics between TMP and the bacteria gives an estimate of the k^{2nd} of *E. coli*, using the value of $k_{^3DOM*}^{TMP}$ as reference. Under the hypothesis that bacteria inactivation is mostly caused by ^{3}DOM*, the k^{2nd} value obtained for *E. coli* with ^{3}DOM*, by using SW-DOM under UV-A irradiation was (1.9 ± 0.1) × 10^{10} M^{-1} s^{-1}, which is very near the k^{2nd} value measured with ACE and AQ2S (see Table 2). The most likely explanation to this finding is that ^{3}AQ2S* and ^{3}SW* have similar ability to inactivate the

bacteria, and that inactivation by irradiated SW is mainly carried out by the triplet states ^{3}SW*. In contrast, with ND it was obtained $k^{2nd} = (5.6 \pm 4.4) \times 10^9$ M^{-1} s^{-1} that is quite far from the target value. This may mean that either the disinfection ability of ^{3}ND* is very different from that of ^{3}AQ2S*, and/or that the disinfection carried out by ND under irradiation also involves an important role of additional transient species (e.g., $^1O_2$ and/or •OH). Interestingly, ND is reported to have a high ability to produce singlet oxygen (Sharpless, 2012).

In order to get insight into the likely role of triplet states and $^1O_2$ in bacteria inactivation with irradiated SW and ND, two systems were tested: the former was purged with N_2 to remove O_2 from the aqueous media, while the latter was left in contact with air in a normal arrangement (no N_2 purging). The normal (air equilibrated) system allows for the combined participation of ^{3}DOM* and $^1O_2$ to the disinfection process. The N_2-purged system was used to determine the interaction with ^{3}DOM* solely. Indeed, in the absence of dissolved O_2 there is no formation of $^1O_2$ while the ^{3}CDOM*-mediated processes are enhanced. The half-life time of ^{3}DOM* in aerated aqueous solutions is in fact in the µs range, while it is around an order of magnitude higher (20–80 µs) in the absence of oxygen (Vione et al., 2014). A comparable issue happens with the steady-state [^{3}DOM*] in the same conditions. A strong inhibition of bacteria inactivation was observed in the presence of ND irradiated under N_2 atmosphere compared to the air-equilibrated system (Figure SM7), which indicates that in this case $^1O_2$ had an important role in *E. coli* inactivation. In contrast to ND, the SW system with N_2 purge was able to cause significant inactivation of bacteria. This finding confirms that the excited triplet state of SW (^{3}SW*) plays an important disinfecting action. Another supportive argument is the higher FFA degradation rate constant observed with ND under UV-A irradiation compared to SW, which suggests higher $^1O_2$ photo-production by ND (see Figure 6A, which also reports for comparison the values of the $^1O_2$ formation quantum yields by ND and SW taken from the literature (Semitsoglou-Tsiapou et al., 2016)). These results agree well with the inferences derived from the discussion of the k^{2nd} values, and the overall findings suggest that the triplet states dominated the inactivation of bacteria in the case of irradiated SW, while $^1O_2$ played an important role in the case of ND. Therefore, a qualitative schematic comparison between SW and ND can be proposed (Figure 6B).

On the other hand, complementary experiments were performed under simulated sunlight, which is relevant to actual SODIS systems (Figure 7 and Text SM4). Competition kinetics to obtain the second-order reaction rate constant for *E. coli* with ^{3}SW* under solar light irradiation was carried out, yielding $k^{2nd} = (2.17 \pm 0.40) \times 10^{10}$

M^{-1} s^{-1}, which is in very good agreement with the value obtained with AQ2S (see Table 2). This confirmed that AQ2S is an excellent DOM proxy in the case of SODIS for *E. coli*.

Finally, in addition to the irradiation of bacteria in the presence of DOM, the photo-Fenton (pF) process with 0.5 ppm Fe^{2+} and 10 ppm H_2O_2 (Eqs. 9-10) was also studied as a source of hydroxyl radicals. pF can be used to improve SODIS in real waters (Ndounla et al., 2013; Sciacca et al., 2010); coherently with literature reports, it was also able to fast inactivate *E. coli* in our system (Figure 7). Interestingly, the second-order reaction rate constant for bacteria and hydroxyl radical from the pF system (k^{2nd} = (1.27 ± 0.45) × 10 $^{11}M^{-1}s^{-1}$) how determined? was similar to the obtained by the photolysis of $NaNO_3$ (Table 2), indicating the good applicability of competition kinetics to the same transient species generated in different ways.

$$Fe^{2+} + H_2O_2 \rightarrow Fe^{3+} + {}^{\bullet}OH + {}^{-}OH \quad (9)$$

$$Fe^{3+} + H_2O + sunlight \rightarrow Fe^{2+} + {}^{\bullet}OH + H^{+} \quad (10)$$

4. Conclusions

We show here that (simulated) sunlight is able to promote significant formation of transient species from specific precursors (i.e., $NaNO_3$, AQ2S and RB), thereby enhancing the photoinduced disinfection of *E. coli*. The studied experimental system also enabled a successful application of the competition kinetics method to determine the second-order inactivation rate constants of the bacteria with hydroxyl radicals, the excited triplet state of AQ2S (here used as DOM proxy), as well as singlet oxygen. These rate constants allow for the modeling of the bacteria inactivation kinetics in outdoor systems (both water bodies and SODIS bottles), but only when the lag phase is over. Indeed, a major difference between bacteria on the one case, and viruses and chemicals on the other is that the photoinactivation of bacteria does not follow a purely first-order kinetics, but a lag phase is observed before the onset of inactivation. Bacteria are in fact able to carry out a certain level of compensation for the photoinduced damage, but at the moment a suitable model approach is not available for the prediction of the bacterial lag time under environmental conditions. The model results suggest that $^1O_2$ plays a minor role in inactivation compared to •OH and ^{3}DOM*, but also that the direct inactivation inside a

SODIS bottle likely plays a more important role than the indirect processes triggered by •OH/^{3}DOM*/$^1O_2$ (which cannot really account for the photoinduced disinfection observed in SODIS systems).

A further series of experiments showed that the UV-A and UV-B components of solar radiation significantly activated DOM for *E. coli* elimination. The strong absorption by organic matter in the UV-A and UV-B regions is known to be associated to the presence of chromophoric and photoactive moieties such as quinones and aromatic carbonyls. Interestingly, the use of humic substances isolated from DOM had a comparable effect on disinfection as DOM itself, but the relevant behavior of humic isolates (unequivocal disinfection enhancement at low TOC, inhibition effects at high TOC) was observed at lower amounts compared to the corresponding DOM. This is a reasonable finding when considering that humic substances are concentrated DOM fractions. Additionally, the comparison between Nordic Lake (ND) and Suwannee river (SW) organic matter showed that in the ND case the photoinduced inactivation was likely carried out by both ^{3}DOM* and $^1O_2$, while ^{3}DOM* alone prevailed in the case of SW. This conclusion was obtained at the qualitative/semi-quantitative level by means of experiments that used competition kinetics with TMP, as well as by comparison of results obtained in aerated systems vs. N_2 atmosphere. Unfortunately, the latter comparison did not allow for a more precise, quantitative differentiation between the ^{3}DOM* and $^1O_2$ pathways. This fact could be associated to an incomplete removal of oxygen from the system or to the intrinsic dependence of $^1O_2$ formation from ^{3}DOM*. Actually, the N_2 atmosphere inhibits $^1O_2$ but enhances ^{3}DOM* at the same time (especially when both $^1O_2$ and ^{3}DOM* are significantly involved in bacteria photoinactivation, as in the case of ND). If one additionally considers that it is not possible to carry out competition kinetics with the $^1O_2$ probe FFA, due to the toxicity of such alcohol to bacteria, the use of individual precursors of transient species (e.g., AQ2S and RB) is a more suitable approach to separately determine the k^{2nd} values with ^{3}DOM* and $^1O_2$. Still, the competition kinetics with TMP in the presence of SW suggested that the k^{2nd} value for *E. coli* obtained with the use of AQ2S was very near the value that could be measured upon SW irradiation. This means that the ability of ^{3}AQ2S* to inactivate bacteria is comparable to that of ^{3}SW* and that, therefore, AQ2S was here a good proxy for SW DOM.

Furthermore, although some preliminary data were obtained concerning the ability of different DOM types to induce *E. coli* disinfection, in order to better understand the role of overall DOM, its origin (autochthonous vs.

allochthonous) and the presence of humic or fulvic acids, more chemical analyses (e.g., NMR, IR) of these substances are required. Chemical characterization of the ketone and quinone group content and structural forms in DOM and humic substances are thus necessary to improve the comprehension of the interaction of these compounds with UV-light and bacteria. Therefore, a comprehensive DOM characterization should be carried out in future works.

5. Acknowledgments

E.A. Serna-Galvis thanks Colciencias for his Ph.D. scholarship (Convocatoria 647 de 2014). EPFL´s authors acknowledge the financial support through the European project WATERSPOUTT H2020-Water-5c-2015 (GA 688928) and the Swiss State Secretariat for Education, Research and Innovation (SEFRI-WATERSPOUTT, No.: 588141). R.A. Torres-Palma thanks Universidad de Antioquia UdeA for the support provided to GIRAB through "Programa de Sostenibilidad" and the financing from Colciencias (Project No 111577757323, Convocatoria 777 de 2017).

6. References

Bodrato, M., Vione, D., 2014. APEX (Aqueous Photochemistry of Environmentally occurring Xenobiotics): a free software tool to predict the kinetics of photochemical processes in surface waters. Environ. Sci. Process. Impacts 16, 732–740. https://doi.org/10.1039/C3EM00541K

Buettner, G.R., Hall, R.D., 1987. Superoxide, Hydrogen-Peroxide and Singlet Oxygen in Hematoporphyrin Derivative-Cysteine, Derivative-Nadh and Derivative-Light Systems. Biochim. Biophys. Acta 923, 501–507. https://doi.org/Doi 10.1016/0304-4165(87)90060-2

Bushaw, K.L., Zepp, R.G., Tarr, M.A., Schulz-Jander, D., Bourbonniere, R.A., Hodson, R.E., Miller, W.L., Bronk, D.A., Moran, M.A., 1996. Photochemical release of biologically available nitrogen from aquatic dissolved organic matter. Nature. https://doi.org/10.1038/381404a0

Buxton, G. V, Greenstock, C.L., Helman, W.P., Ross, A.B., 1988. Critical-review of rate constants for reactions of hydrated electrons, hydrogen-atoms and hydroxyl radicals (.OH/.O-) in aqueous-solution. J. Phys. Chem. Ref. Data. https://doi.org/10.1063/1.555805

Chen, J., Gu, B., LeBoeuf, E.J., Pan, H., Dai, S., 2002. Spectroscopic characterization of the structural and functional properties of natural organic matter fractions. Chemosphere 48, 59–68. https://doi.org/10.1016/S0045-6535(02)00041-3

D'Andrilli, J., Foreman, C.M., Marshall, A.G., Mcknight, D.M., 2013. Organic Geochemistry Characterization of IHSS Pony Lake fulvic acid dissolved organic matter by electrospray ionization Fourier transform ion cyclotron resonance mass spectrometry and fluorescence spectroscopy. Org. Geochem. 65, 19–28. https://doi.org/10.1016/j.orggeochem.2013.09.013

Desmond-Le Quéméner, E., Bouchez, T., 2014. A thermodynamic theory of microbial growth. ISME J. 8, 1747–1751. https://doi.org/10.1038/ismej.2014.7

Fernàndez-Ibañez, P., McGuigan, K.G., Fatta-Kassinos, D., 2017. Can solar water-treatment really help in the fight against water shortages? Europhys. News 48, 26–30. https://doi.org/10.1051/epn/2017304

Fisher, M.B., Love, D.C., Schuech, R., Nelson, K.L., 2011. Simulated Sunlight Action Spectra for Inactivation of MS2 and PRD1 Bacteriophages in Clear Water. Environ. Sci. Technol. 45, 9249–9255. https://doi.org/10.1021/es201875x

Giannakis, S., Darakas, E., Escalas-Cañellas, A., Pulgarin, C., 2015. Environmental considerations on solar disinfection of wastewater and the subsequent bacterial (re)growth. Photochem. Photobiol. Sci. 14, 618–625. https://doi.org/10.1039/c4pp00266k

Giannakis, S., López, M.I.P., Spuhler, D., Pérez, J.A.S., Ibáñez, P.F., Pulgarin, C., 2016a. Solar disinfection is an augmentable, in situ-generated photo-Fenton reaction-Part 2: A review of the applications for drinking water and wastewater disinfection. Appl. Catal. B Environ. 198, 431–446. https://doi.org/10.1016/j.apcatb.2016.06.007

Giannakis, S., Polo López, M.I., Spuhler, D., Sánchez Pérez, J.A., Fernández Ibáñez, P., Pulgarin, C., 2016b. Solar disinfection is an augmentable, in situ-generated photo-Fenton reaction—Part 1: A review of the mechanisms and the fundamental aspects of the process. Appl. Catal. B Environ. 199, 199–223. https://doi.org/10.1016/j.apcatb.2016.06.009

Giannakis, S., Rtimi, S., Darakas, E., Escalas-Canellas, A., Pulgarin, C., 2015. Light wavelength-dependent E. coli survival changes after simulated solar disinfection of secondary effluent. Photochem. Photobiol. Sci. 14, 2238–2250. https://doi.org/10.1039/C5PP00110B

Giannakis, S., Voumard, M., Rtimi, S., Pulgarin, C., 2018. Bacterial disinfection by the photo-Fenton process: Extracellular oxidation or intracellular photo-catalysis? Appl. Catal. B Environ. 227, 285–295. https://doi.org/https://doi.org/10.1016/j.apcatb.2018.01.044

Golanoski, K.S., Fang, S., Del Vecchio, R., Blough, N. V., 2012. Investigating the mechanism of phenol photooxidation by humic substances. Environ. Sci. Technol. 46, 3912–3920. https://doi.org/10.1021/es300142y

Halladja, S., Ter Halle, A., Aguer, J.P., Boulkamh, A., Richard, C., 2007. Inhibition of humic substances mediated photooxygenation of furfuryl alcohol by 2,4,6-trimethylphenol. Evidence for reactivity of the phenol with humic triplet excited states. Environ. Sci. Technol. 41, 6066–6073. https://doi.org/10.1021/es070656t

International Humic Substances Society, 2018. IHSS web site [WWW Document]. URL http://humic-substances.org/#products (accessed 1.16.18).

Kochevar, I.E., Redmond, R.W., 2000. Photosensitized production of single oxygen. Methods Enzymol. 319, 20–28. https://doi.org/10.1016/S0076-6879(00)19004-4

Kohn, T., Mattle, M.J., Minella, M., Vione, D., 2016. A modeling approach to estimate the solar disinfection of viral indicator organisms in waste stabilization ponds and surface waters. Water Res. 88, 912–922. https://doi.org/10.1016/j.watres.2015.11.022

Kohn, T., Nelson, K.L., 2007. Sunlight-mediated inactivation of MS2 coliphage via exogenous singlet oxygen produced by sensitizers in natural waters. Environ. Sci. Technol. 41, 192–197. https://doi.org/10.1021/es061716i

Loeff, I., Treinin, A., Linschitz, H., 1984. The photochemistry of 9,10-anthraquinone-2-sulfonate in solution. 2. Effects of inorganic anions: quenching vs. radical formation at moderate and high anion concentrations. J. Phys. Chem. 88, 4931–4937. https://doi.org/10.1021/j150665a028

Mack, J., Bolton, J.R., 1999. Photochemistry of nitrite and nitrate in aqueous solution: a review. J. Photochem. Photobiol. A Chem. 128, 1–13. https://doi.org/10.1016/S1010-6030(99)00155-0

Maddigapu, P.R., Bedini, A., Minero, C., Maurino, V., Vione, D., Brigante, M., Mailhot, G., Sarakha, M., 2010. The pH-dependent photochemistry of anthraquinone-2-sulfonate. Photochem. Photobiol. Sci. 9, 323. https://doi.org/10.1039/b9pp00103d

Mangayayam, M., Kiwi, J., Giannakis, S., Pulgarin, C., Zivkovic, I., Magrez, A., Rtimi, S., 2017. FeOx magnetization enhancing E. coli inactivation by orders of magnitude on Ag-TiO2 nanotubes under sunlight. Appl. Catal. B Environ. 202, 438–445. https://doi.org/10.1016/j.apcatb.2016.09.064

Maraccini, P.A., Wenk, J., Boehm, A.B., 2016a. Photoinactivation of Eight Health-Relevant Bacterial Species: Determining the Importance of the Exogenous Indirect Mechanism. Environ. Sci. Technol. 50, 5050–5059. https://doi.org/10.1021/acs.est.6b00074

Maraccini, P.A., Wenk, J., Boehm, A.B., 2016b. Exogenous indirect photoinactivation of bacterial pathogens and indicators in water with natural and synthetic photosensitizers in simulated sunlight with reduced UVB. J. Appl. Microbiol. 121, 587–597. https://doi.org/10.1111/jam.13183

Mattle, M.J., Vione, D., Kohn, T., 2015. Conceptual model and experimental framework to determine the contributions of direct and indirect photoreactions to the solar disinfection of MS2, phiX174, and adenovirus. Environ. Sci. Technol. 49, 334–342. https://doi.org/10.1021/es504764u

McGuigan, K.G., Conroy, R.M., Mosler, H.J., du Preez, M., Ubomba-Jaswa, E., Fernandez-Ibañez, P., 2012.

Solar water disinfection (SODIS): A review from bench-top to roof-top. J. Hazard. Mater. 235–236, 29–46. https://doi.org/10.1016/j.jhazmat.2012.07.053

Minella, M., Giannakis, S., Mazzavillani, A., Maurino, V., Minero, C., Vione, D., 2017. Phototransformation of Acesulfame K in surface waters: Comparison of two techniques for the measurement of the second-order rate constants of indirect photodegradation, and modelling of photoreaction kinetics. Chemosphere 186, 185–192. https://doi.org/10.1016/j.chemosphere.2017.07.128

Ndounla, J., Kenfack, S., Wéthé, J., Pulgarin, C., 2014. Relevant impact of irradiance (vs . dose) and evolution of pH and mineral nitrogen compounds during natural water disinfection by photo-Fenton in a solar CPC reactor. "Applied Catal. B, Environ. 148–149, 144–153. https://doi.org/10.1016/j.apcatb.2013.10.048

Ndounla, J., Spuhler, D., Kenfack, S., Wéthé, J., Pulgarin, C., 2013. Inactivation by solar photo-Fenton in pet bottles of wild enteric bacteria of natural well water: Absence of re-growth after one week of subsequent storage. Appl. Catal. B Environ. 129, 309–317. https://doi.org/10.1016/j.apcatb.2012.09.016

Nguyen, M.T., 2015. Thesis: Sunlight inactivation of fecal indicator bacteria in open-water unit process wetlands. University of California, Berkeley.

Pubchem, 2018. 2,4,6-Trimethylphenol properties [WWW Document]. URL https://pubchem.ncbi.nlm.nih.gov/compound/2_4_6-trimethylphenol#section=Top (accessed 1.16.18).

Rincón, A.-G., Pulgarin, C., 2004. Bactericidal action of illuminated TiO2 on pure Escherichia coli and natural bacterial consortia: post-irradiation events in the dark and assessment of the effective disinfection time. Appl. Catal. B Environ. 49, 99–112. https://doi.org/https://doi.org/10.1016/j.apcatb.2003.11.013

Rodríguez, F.J., Schlenger, P., García-Valverde, M., 2016. Monitoring changes in the structure and properties of humic substances following ozonation using UV-Vis, FTIR and 1H NMR techniques. Sci. Total Environ. 541, 623–637. https://doi.org/10.1016/j.scitotenv.2015.09.127

Romero-Maraccini, O.C., Sadik, N.J., Rosado-Lausell, S.L., Pugh, C.R., Niu, X.Z., Croué, J.P., Nguyen, T.H., 2013. Sunlight-induced inactivation of human Wa and porcine OSU rotaviruses in the presence of

exogenous photosensitizers. Environ. Sci. Technol. 47, 11004–11012. https://doi.org/10.1021/es402285u

Romero, O.C., Straub, A.P., Kohn, T., Nguyen, T.H., 2011. Role of temperature and suwannee river natural organic matter on inactivation kinetics of rotavirus and bacteriophage MS2 by solar irradiation. Environ. Sci. Technol. 45, 10385–10393. https://doi.org/10.1021/es202067f

Rosado-Lausell, S.L., Wang, H., Gutiérrez, L., Romero-Maraccini, O.C., Niu, X.Z., Gin, K.Y.H., Croué, J.P., Nguyen, T.H., 2013. Roles of singlet oxygen and triplet excited state of dissolved organic matter formed by different organic matters in bacteriophage MS2 inactivation. Water Res. 47, 4869–4879. https://doi.org/10.1016/j.watres.2013.05.018

Sciacca, F., Rengifo-Herrera, J.A., Wéthé, J., Pulgarin, C., 2011. Solar disinfection of wild Salmonella sp. in natural water with a 18L CPC photoreactor: Detrimental effect of non-sterile storage of treated water. Sol. Energy 85, 1399–1408. https://doi.org/10.1016/j.solener.2011.03.022

Sciacca, F., Rengifo-Herrera, J.A., Wéthé, J., Pulgarin, C., 2010. Dramatic enhancement of solar disinfection (SODIS) of wild Salmonella sp. in PET bottles by H2O2 addition on natural water of Burkina Faso containing dissolved iron. Chemosphere 78, 1186–1191. https://doi.org/10.1016/j.chemosphere.2009.12.001

Semitsoglou-Tsiapou, S., Mous, A., Templeton, M.R., Graham, N.J.D., Hernández Leal, L., Kruithof, J.C., 2016. The role of natural organic matter in nitrite formation by LP-UV/H2O2 treatment of nitrate-rich water. Water Res. 106, 312–319. https://doi.org/10.1016/j.watres.2016.10.001

Sharpless, C.M., 2012. Lifetimes of triplet dissolved natural organic matter (DOM) and the effect of NaBH4 reduction on singlet oxygen quantum yields: Implications for DOM photophysics. Environ. Sci. Technol. 46, 4466–4473. https://doi.org/10.1021/es300217h

Sharpless, C.M., Blough, N. V., 2014. The importance of charge-transfer interactions in determining chromophoric dissolved organic matter (CDOM) optical and photochemical properties. Environ. Sci. Process. Impacts 16, 654–671. https://doi.org/10.1039/C3EM00573A

Silverman, A.I., Nguyen, M.T., Schilling, I.E., Wenk, J., Nelson, K.L., 2015. Sunlight Inactivation of Viruses in Open-Water Unit Process Treatment Wetlands: Modeling Endogenous and Exogenous Inactivation Rates. Environ. Sci. Technol. 49, 2757–2766. https://doi.org/10.1021/es5049754

Sinton, L.W., Hall, C.H., Lynch, P. a, Davies-Colley, R.J., 2002. Sunlight Inactivation of Fecal Indicator Bacteria and Bacteriophages from Waste Stabilization Pond Effluent in Fresh and Saline Waters Sunlight Inactivation of Fecal Indicator Bacteria and Bacteriophages from Waste Stabilization Pond Effluent in Fresh and. Appl. Environ. Microbiol. 68, 1122–1131. https://doi.org/10.1128/AEM.68.3.1122

Spuhler, D., Rengifo-Herrera, J., Pulgarín, C., 2010. Environmental The effect of Fe2+, Fe3+, H2O2 and the photo-Fenton reagent at near neutral pH on the solar disinfection (SODIS) at low temperatures of water containing Escherichia coli K12. Appl. Catal. B Environ. 96, 126–141. https://doi.org/10.1016/j.apcatb.2010.02.010

Thompson, C.L., Sancar, A., 2002. Photolyase/cryptochrome blue-light photoreceptors use photon energy to repair DNA and reset the circadian clock. Oncogene 21, 9043–9056. https://doi.org/10.1038/sj.onc.1205958

Vione, D., Falletti, G., Maurino, V., Minero, C., Pelizzetti, E., Malandrino, M., Ajassa, R., Olariu, R.-I., Arsene, C., 2006. Sources and Sinks of Hydroxyl Radicals upon Irradiation of Natural Water Samples. Environ. Sci. Technol. 40, 3775–3781. https://doi.org/10.1021/es052206b

Vione, D., Minella, M., Maurino, V., Minero, C., 2014. Indirect photochemistry in sunlit surface waters: Photoinduced production of reactive transient species. Chem. - A Eur. J. 20, 10590–10606. https://doi.org/10.1002/chem.201400413

Walpen, N., Schroth, M.H., Sander, M., 2016. Quantification of Phenolic Antioxidant Moieties in Dissolved Organic Matter by Flow-Injection Analysis with Electrochemical Detection. Environ. Sci. Technol. 50, 6423–6432. https://doi.org/10.1021/acs.est.6b01120

Abbreviations list:

ACE: acesulfame K; AQ2S: anthraquinone-2-sulfonate; BL: blue light; DOM: dissolved organic matter; ^{3}DOM*: triplet excited state of organic matter; EDC: electron donating capability; E_{365}: molar absorptivity at 365 nm; FFA: furfuryl alcohol; GL: green light; k^{1}: pseudo-first order rate constant; k^{2nd}: second order inactivation rate constant; ND: Nordic lake organic matter; pF: photo-Fenton process; PLFA: Pony lake fulvic acid; RB: rose bengal; SODIS: solar disinfection; SW: Suwannee river organic matter; SWHA: Suwannee river humic acid; SWFA: Suwannee river fulvic acid; TMP: 2,4,6-trimethylphenol; UV: ultraviolet light; YL: yellow light.

Figure captions

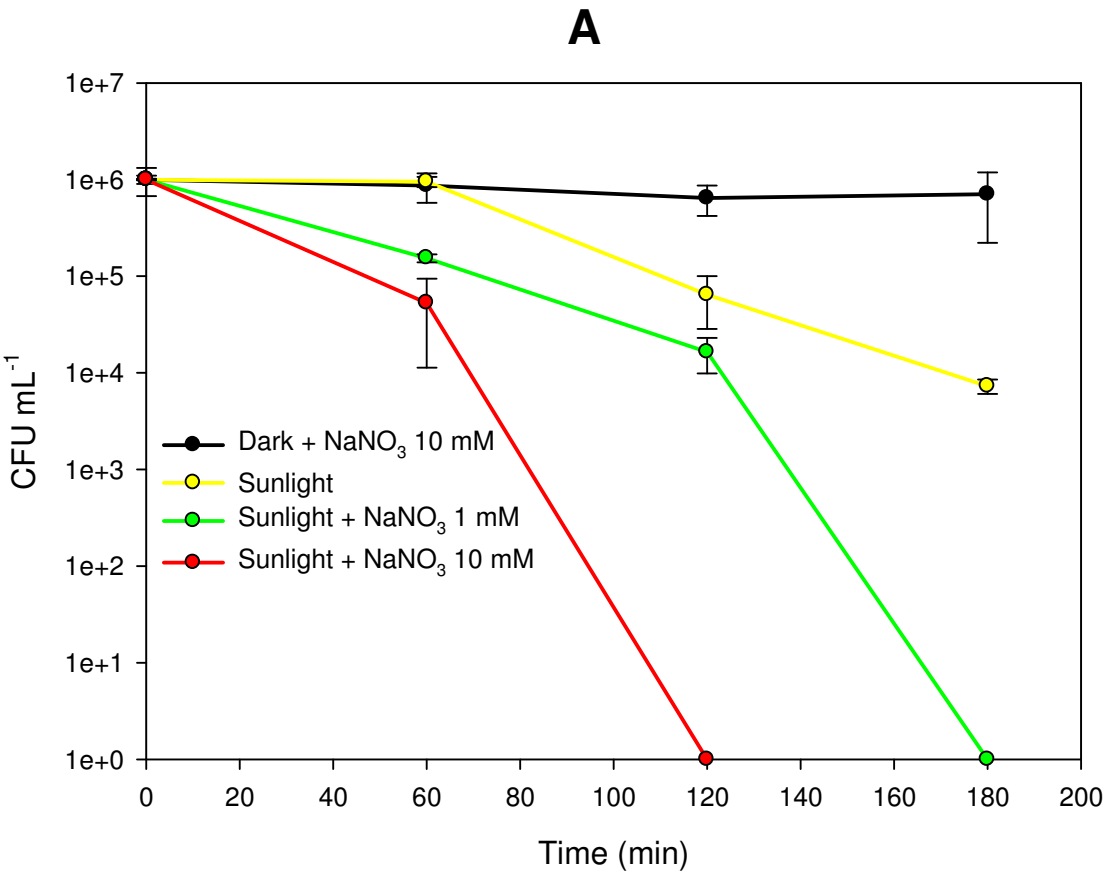

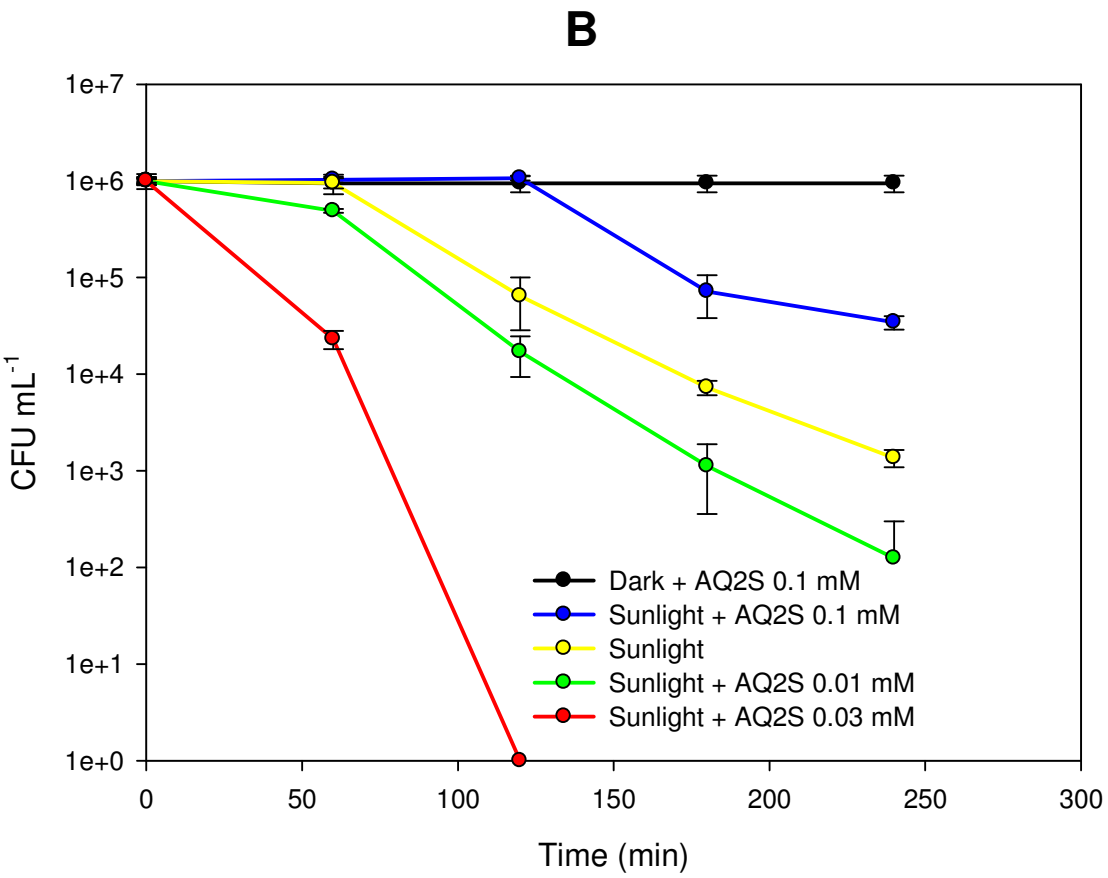
B
1e+7
1e+6
1e+5
1e+4
1e+3
1e+2
1e+1
1e+0
CFU mL-1
0
50
100
150
200
250
300
Time (min)
Dark + AQ2S 0.1 mM
Sunlight + AQ2S 0.1 mM
Sunlight
Sunlight + AQ2S 0.01 mM
Sunlight + AQ2S 0.03 mM

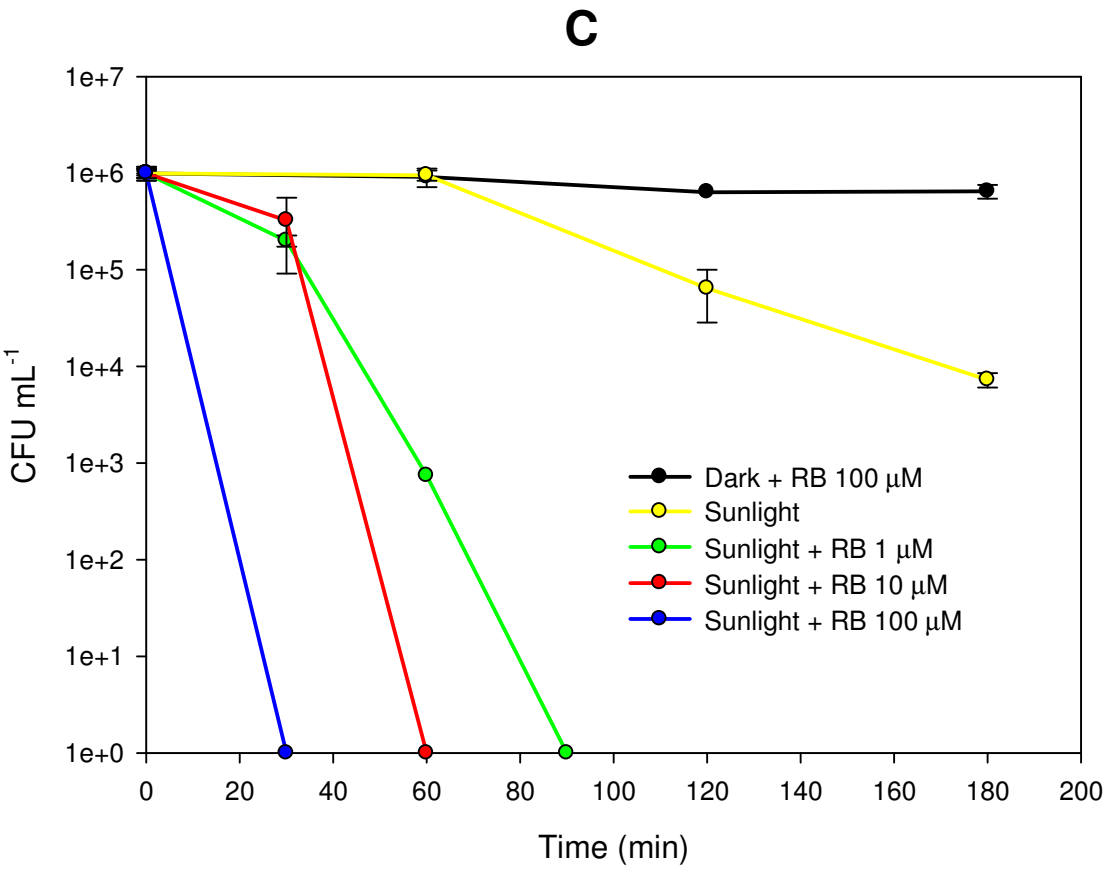
C
1e+7
1e+6
1e+5
1e+4
1e+3
1e+2
1e+1
1e+0
CFU mL-1
0
20
40
60
80
100
120
140
160
180
200
Time (min)
Dark + RB 100 µM
Sunlight
Sunlight + RB 1 µM
Sunlight + RB 10 µM
Sunlight + RB 100 µM

Figure 1. *E. coli* inactivation using simulated solar light and different concentrations of specific precursors of transient species. **A.** Sodium nitrate ($NaNO_3$) as •OH source. **B.** Anthraquinone-2-sulfonate (AQ2S) as ^{3}AQ2S* source. **C.** Rose Bengal (RB) as $^1O_2$ source. Simulated sunlight irradiance: 600 W/m^2. ***Note:*** Here, complete disinfection means that there was no observed bacterial growth on the plates at any dilution. However, because in exponential scale the zero does not exit, 1e+0 value is used to represent that the bacterial population reaches zero.

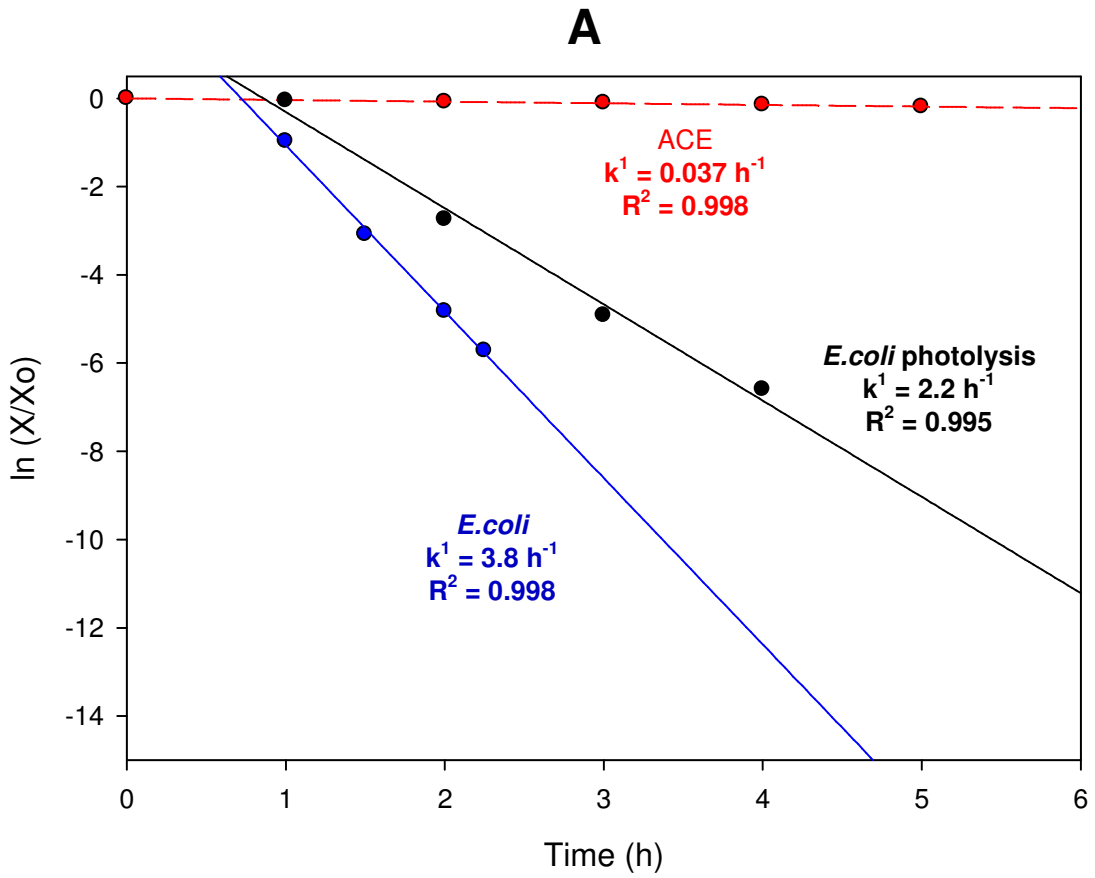
A
ln (X/Xo)
Time (h)
0
-2
-4
-6
-8
-10
-12
-14
0
1
2
3
4
5
6
ACE
k1 = 0.037 h-1
R2 = 0.998
E.coli photolysis
k1 = 2.2 h-1
R2 = 0.995
E.coli
k1 = 3.8 h-1
R2 = 0.998

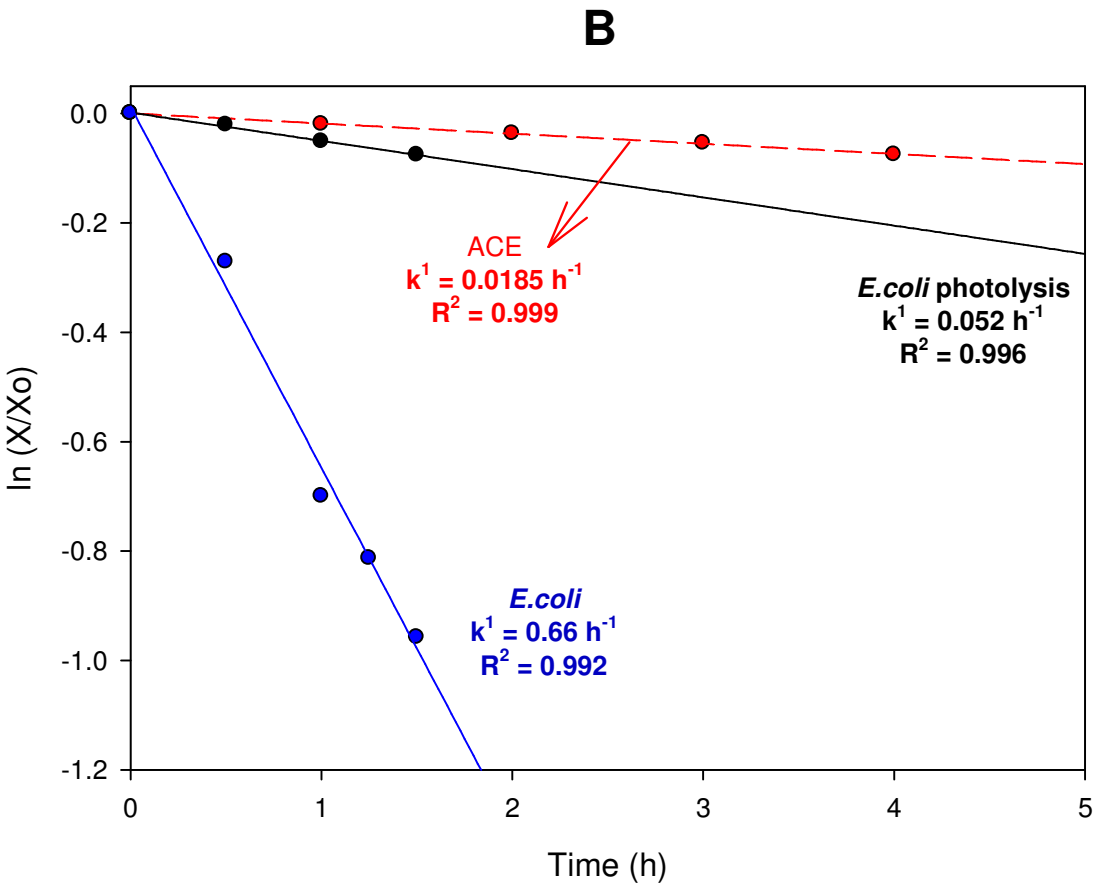
B
0.0
-0.2
-0.4
-0.6
-0.8
-1.0
-1.2
ln (X/Xo)
0
1
2
3
4
5
Time (h)
ACE
k1 = 0.0185 h-1
R2 = 0.999
E.coli photolysis
k1 = 0.052 h-1
R2 = 0.996
E.coli
k1 = 0.66 h-1
R2 = 0.992

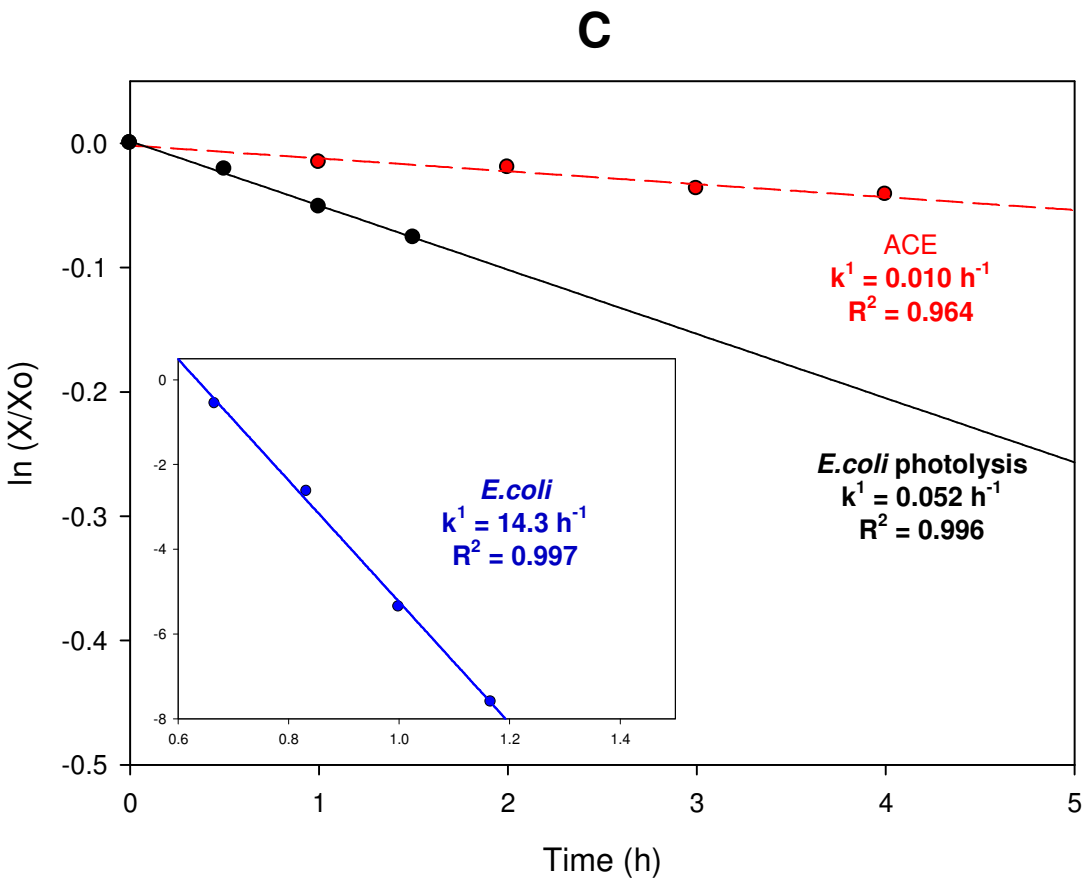

Figure 2. Competition kinetics between acesulfame K (ACE) and *E. coli* for (**A**) •OH, (**B**) ^{3}AQ2S* and (**C**) $^{1}O_2$. Sunlight intensity: 600 W/m^2; [E. coli]: 10^6 CFU mL^{-1}, [ACE]: 10 µM, [NaNO3]: 10mM, [AQ2S]: 0.03mM and [RB]: 10 µM.

Note: the k^1 value for *E. coli* in Figure 2A is determined after the lag-phase has stopped, because the existence of a lag period prevents the whole trend of *ln(X/Xo) vs. Time* to be linear. Therefore, the relevant trend lines for bacteria do not start from the point (ln(X/Xo),Time) = (0,0). Moreover, due to the direct disinfection carried out by solar light, the k^1 value associated to direct bacteria photoinactivation had to be subtracted from the k^1 observed with irradiated $NaNO_3$. The latter does in fact take into account both the direct inactivation and the •OH action on bacteria.

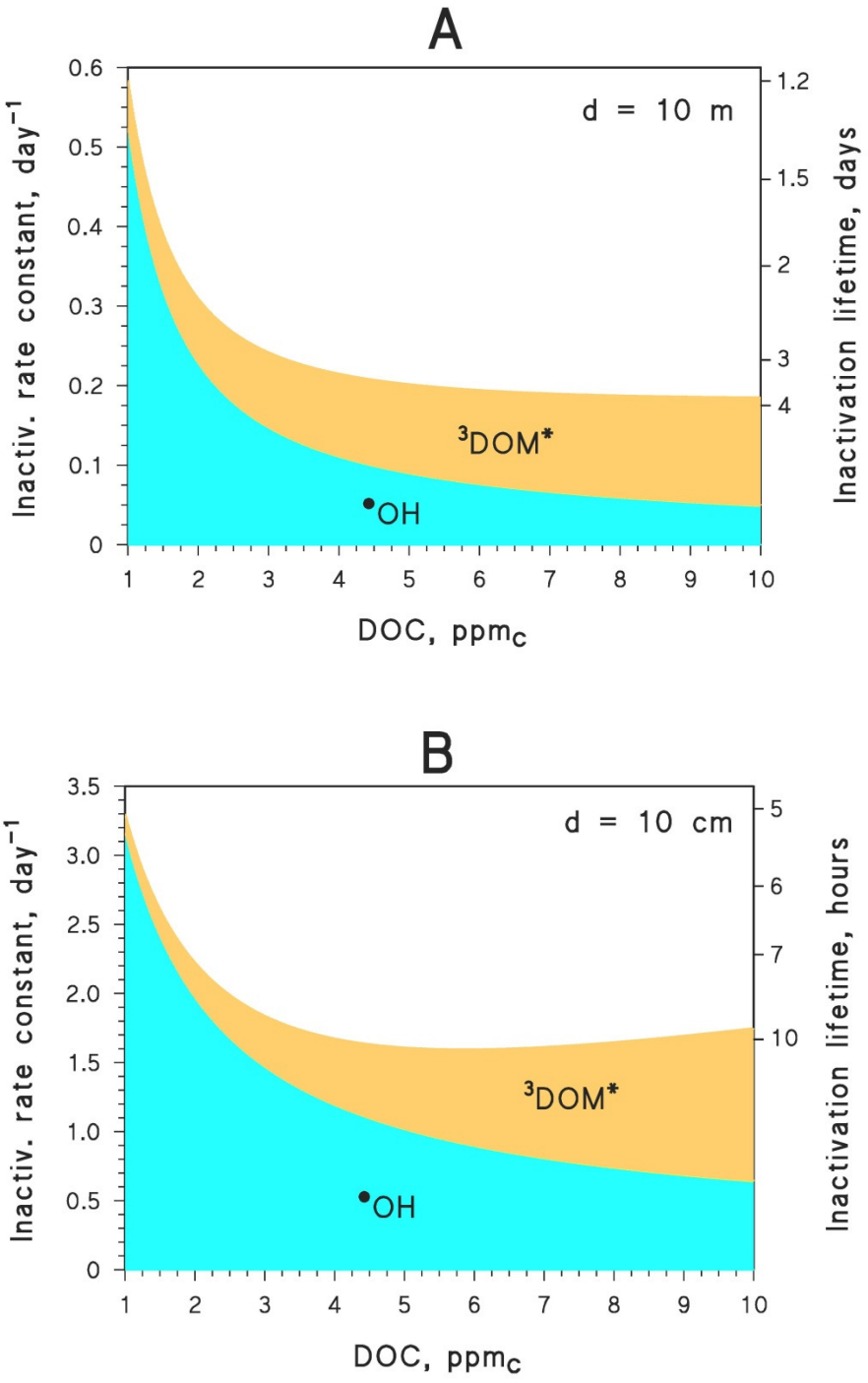

Figure 3. Modeled inactivation rate constants (left Y-axis) and corresponding lifetimes (right Y-axis) for *E. coli*, as a function of the dissolved organic carbon (DOC), for water depths d of **(A)** 10 m and **(B)** 10 cm. Both the overall inactivation kinetics and the contribution of the main processes ($^{\bullet}OH$ and $^{3}DOM^{*}$, while $^{1}O_2$ plays a

negligible role) are reported on the plot. Other water conditions: 0.1 mM nitrate, 1 μM nitrite, 1 mM bicarbonate, 10 μM carbonate. ***Note:*** the direct inactivation is not considered here.

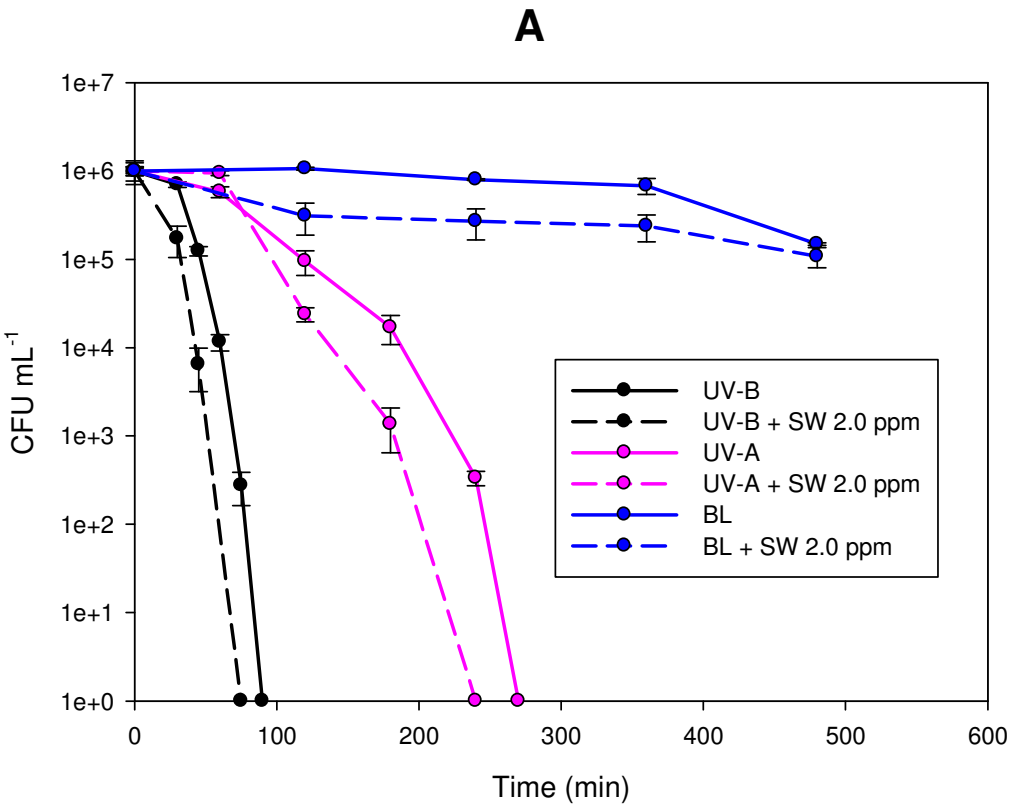
A
1e+7
1e+6
1e+5
1e+4
1e+3
1e+2
1e+1
1e+0
CFU mL-1
0
100
200
300
400
500
600
Time (min)
UV-B
UV-B + SW 2.0 ppm
UV-A
UV-A + SW 2.0 ppm
BL
BL + SW 2.0 ppm

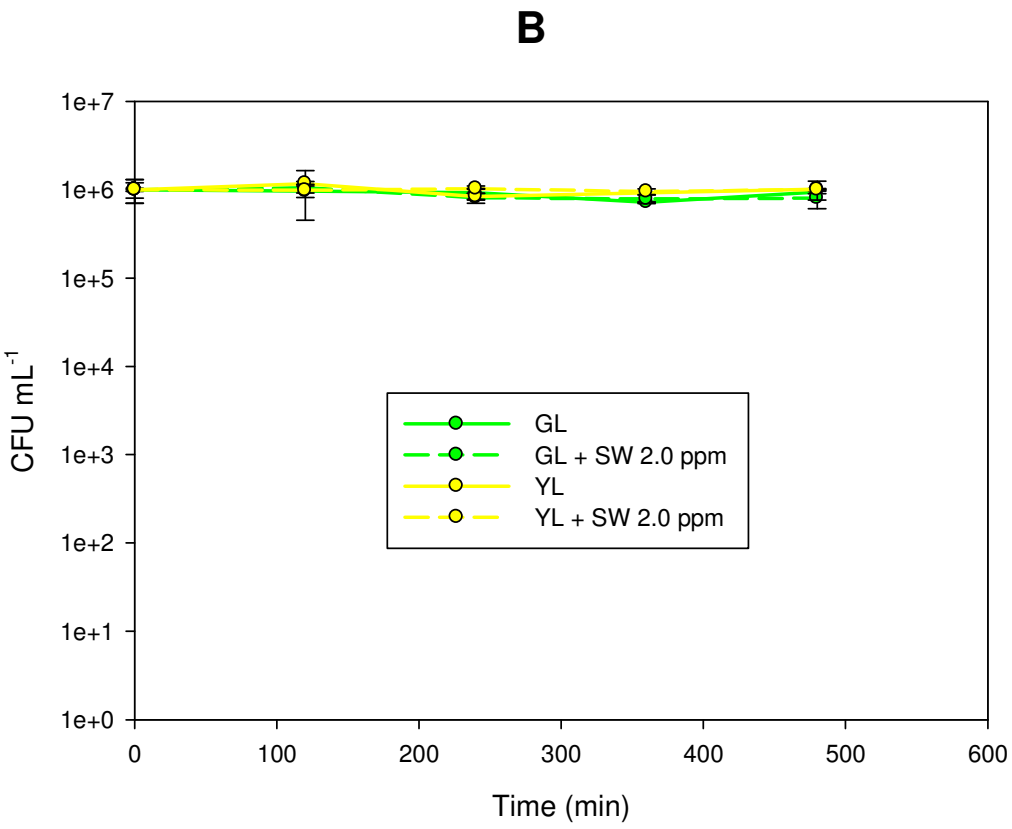
B
1e+7
1e+6
1e+5
1e+4
1e+3
1e+2
1e+1
1e+0
CFU mL-1
0
100
200
300
400
500
600
Time (min)
GL
GL + SW 2.0 ppm
YL
YL + SW 2.0 ppm

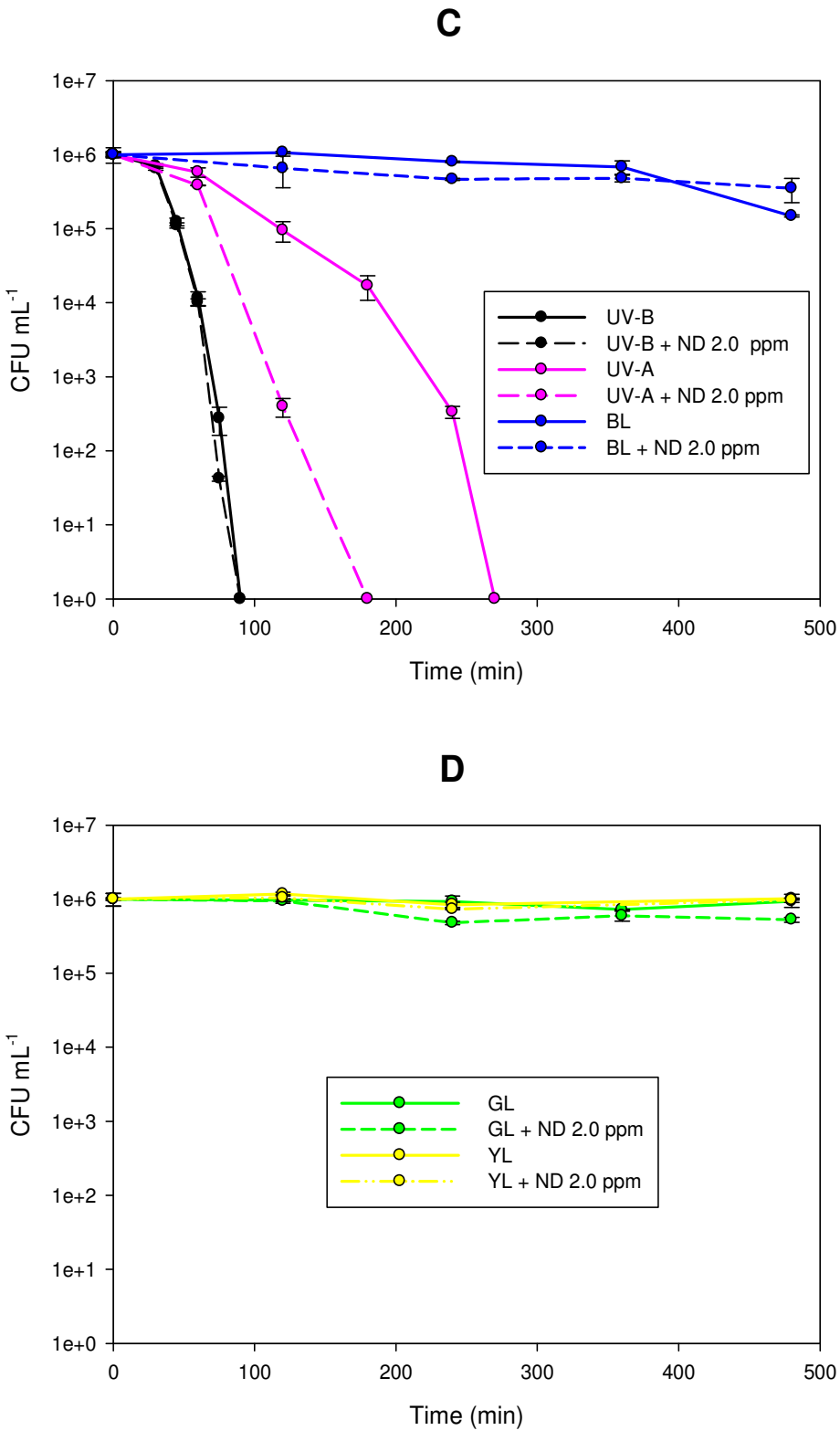

Figure 4. Effect of light type on DOM activation for *E. coli* elimination. **A.** UV-B, UV-A and Blue light (BL) with and without SW. **B.** Green light (GL) and Yellow light (YL) with and without SW. **C.** UV-B, UV-A and

Blue light (BL) with and without ND. **D.** Green light (GL) and Yellow light (YL) with and without ND. All systems were operated at an irradiance of 40 ± 2 W/m^2.

A

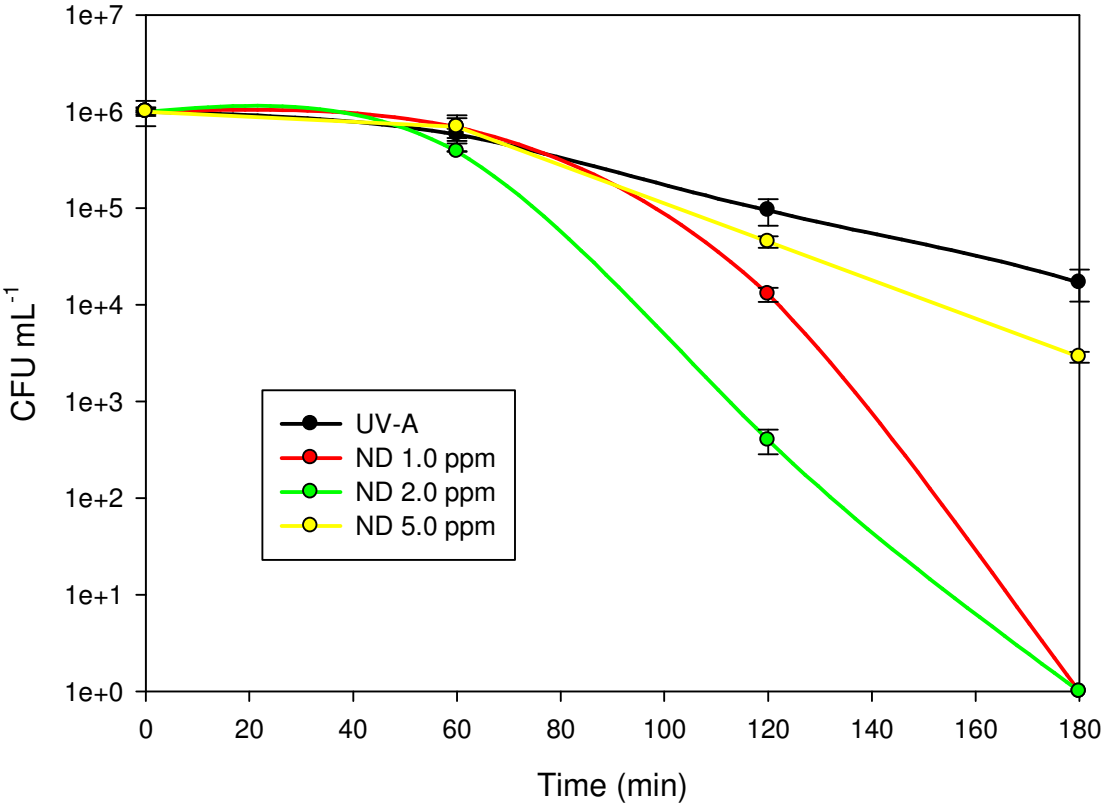
1e+7
1e+6
1e+5
1e+4
1e+3
1e+2
1e+1
1e+0
CFU mL-1
0
20
40
60
80
100
120
140
160
180
Time (min)
UV-A
ND 1.0 ppm
ND 2.0 ppm
ND 5.0 ppm

B

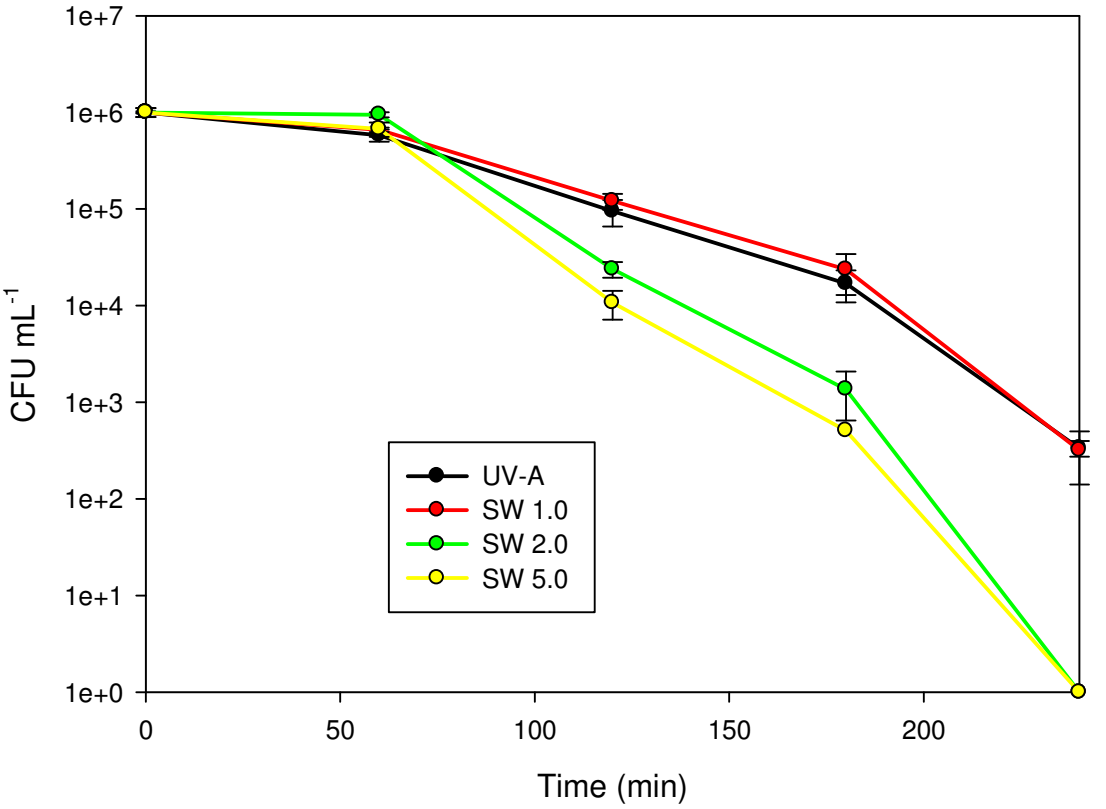
1e+7
1e+6
1e+5
1e+4
1e+3
1e+2
1e+1
1e+0
CFU mL-1
0
50
100
150
200
Time (min)
UV-A
SW 1.0
SW 2.0
SW 5.0

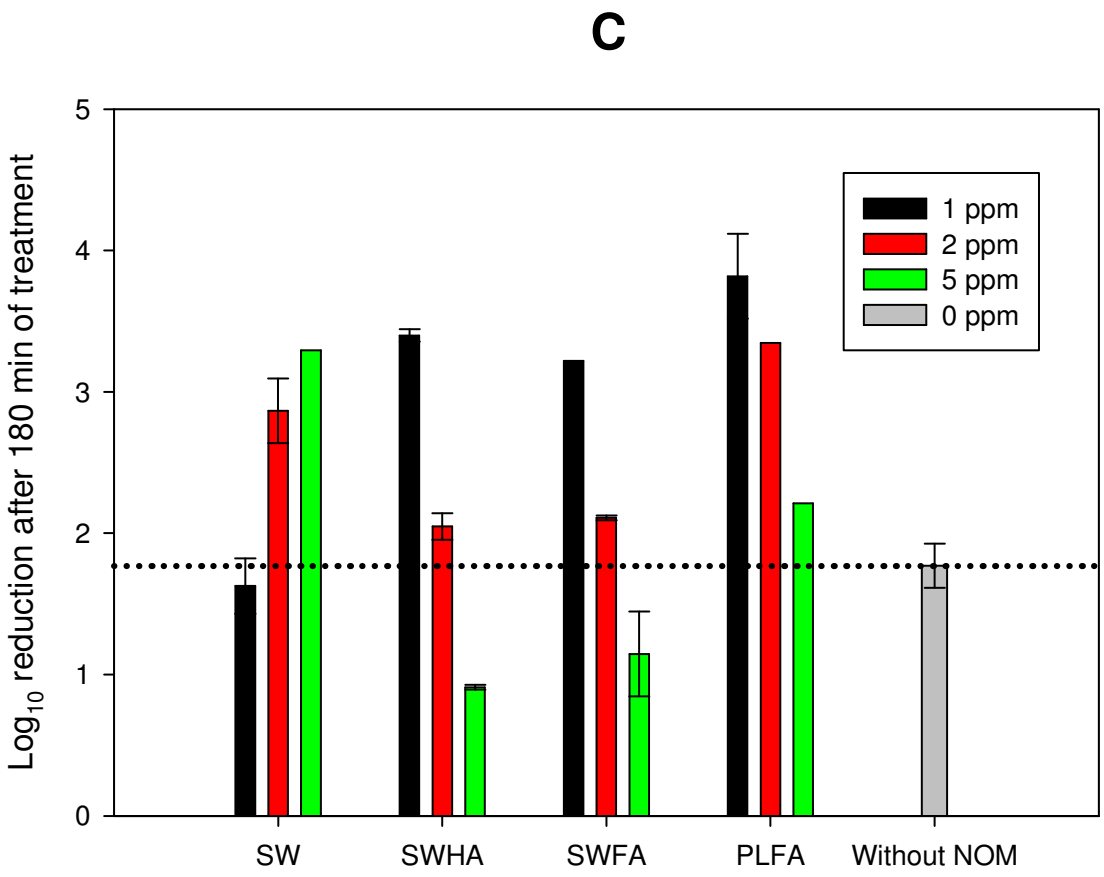

Figure 5. *E. coli* inactivation using UV-A radiation and different organic matter specimens at different concentrations. **A.** Nordic lake NOM (ND). **B.** Suwannee river NOM (SW). **C.** Comparison among different specimens of DOM and humic substances. UV-A irradiance: 40 ± 2 W/m^2.

A

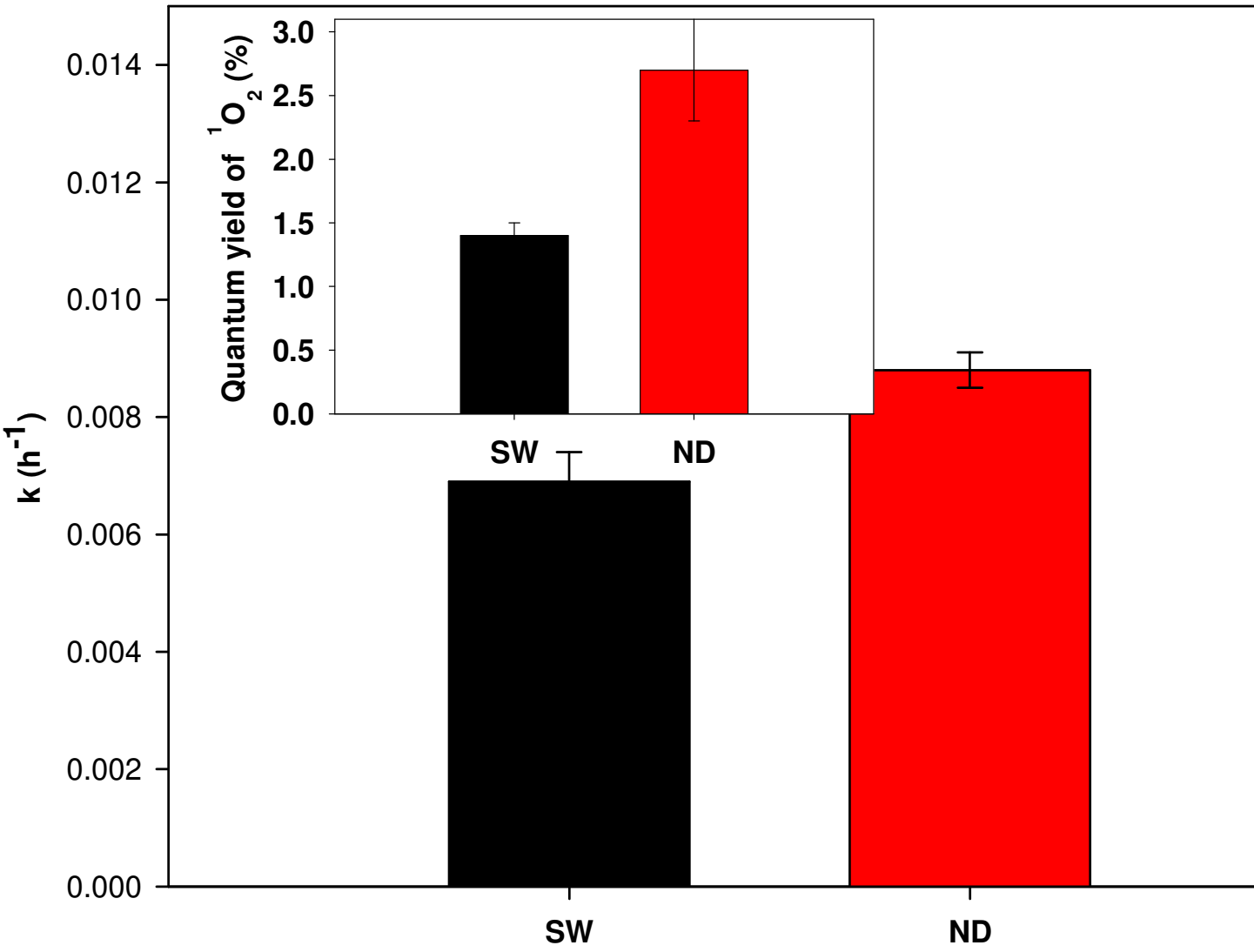
k (h-1)
0.014
0.012
0.010
0.008
0.006
0.004
0.002
0.000
SW
ND
Quantum yield of 1O2 (%)
3.0
2.5
2.0
1.5
1.0
0.5
0.0
SW
ND

B

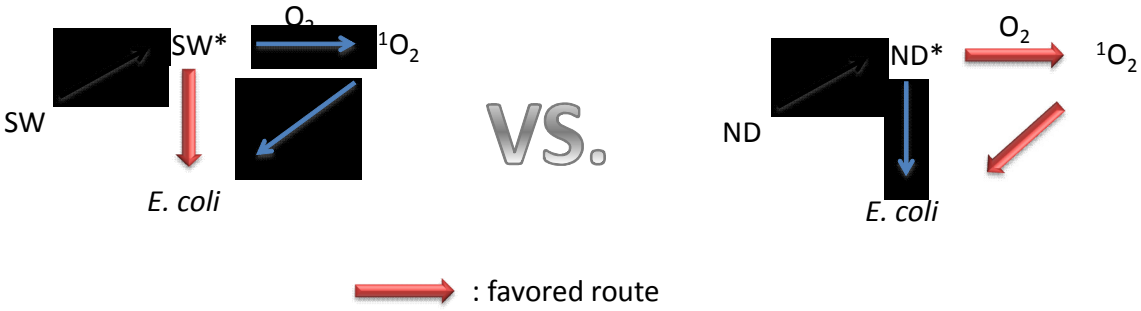

Figure 6. **A.** First-order reaction rate constants (k) for the elimination of furfuryl alcohol (FFA, 0.05 mM) in bacteria absence by NOM (SW or ND, 2.0 ppm TOC), under UV-A light (40 ± 2 W/m^2 irradiance). *Inset*: Quantum yield for singlet oxygen production (Adapted from (Sharpless, 2012)). **B.** Qualitative scheme of the DOM action on *E. coli* in systems exposed to UV-A radiation.

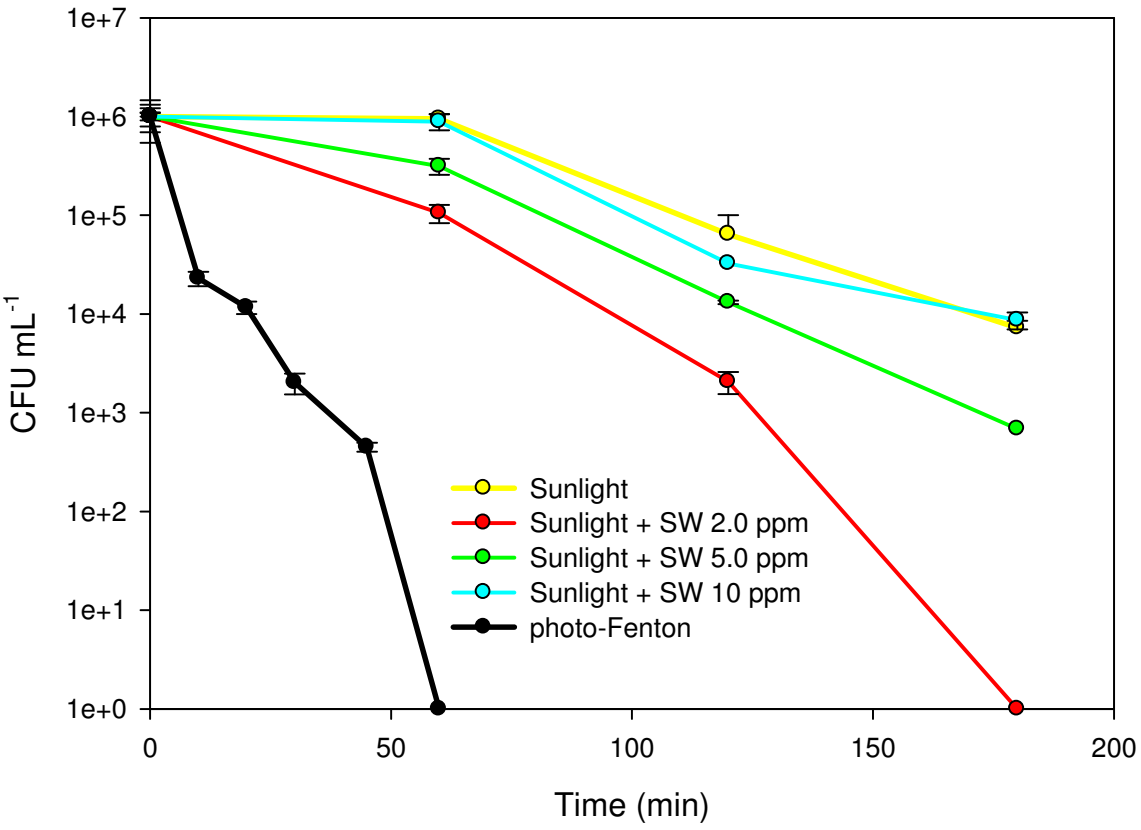

Figure 7. SODIS in the presence of SW at different concentrations: 0, 1, 2 and 5 ppm TOC. Photo-Fenton system: [Fe^{2+}]: 0.5 ppm; [H_2O_2]: 10 ppm. Global irradiance of simulated sunlight: 600W/m^2.

Table captions

Table 1. Chromatographic conditions for the compounds analyses

Compound	**Elution mode**	**Flow rate (mL min^{-1})/ run time (min)/ retention time (min)**	**Detection wavelength (nm)**
ACE	Isocratic Acetonitrile/Water 30%/70%	0.6/10/4.5	224
TMP	Isocratic Acetonitrile/Water 50%/50%	1/15/13.1	278
FFA	Isocratic Acetonitrile/Water 30%/70%	0.8/10/5.2	215

Table 2. Second order reaction rate constants (k^{2nd}) between *E. coli* and the photogenerated transient species.

Transient Species	**•OH**	**^{3}AQ2S***	**$^1O_2$**
$\mathbf{k^{2nd}}_{ACE}$ in $M^{-1}\ s^{-1}$ (*)	$(5.9 \pm 2.0) \times 10^9$	$(5.5 \pm 2.2) \times 10^8$	$(2.8 \pm 1.1) \times 10^4$
$\mathbf{k^{2nd}}_{E.\ coli}$ in $M^{-1}\ s^{-1}$	$(2.5 \pm 0.9) \times 10^{11}$	$(1.8 \pm 0.7) \times 10^{10}$	$(3.8 \pm 1.6) \times 10^7$

(*) Values from Minella et al. (Minella et al., 2017).

Table 3. Indicative photo-chemical properties of the tested DOM and humic substances.

Substance	**E_{365nm}** (M^{-1} cm^{-1}) Measured	**Phenolic content** (meq gC^{-1}) (International Humic Substances Society, 2018)	**EDC** (μmol_{e^-} mL^{-1}) (Walpen et al., 2016)
SW	58.84	2.47	0.9
ND	68.82	---	---
SWHA	162.04	3.72	1.4
SWFA	75.58	2.91	1.4
PLFA	43.78	1.75	0.7

---: Not reported.

Note: E_{365nm} (units of M^{-1} cm^{-1}) is the molar absorption coefficient at 365 nm (measured over an optical path length of 1 cm). This parameter reflects the ability of the studied DOM samples to absorb UV-A radiation. On the other hand, the phenolic content (units of meq gC^{-1}) and the electron donating capability (EDC, units of μmol_{e^-} mL^{-1}) are indicators of the photochemical response of DOM to light (International Humic Substances Society, 2018; Sharpless and Blough, 2014; Walpen et al., 2016).